SILYMARIN LOADED SUPER PARAMAGNETIC IRON OXIDE NANOPARTICLE (SPIONS) FOR TARGETING SARS COV-2 TO COMBAT COVID-19

A Dissertation submitted to

THE TAMIL NADU Dr. M.G.R. MEDICAL UNIVERSITY

CHENNAI – 600 032

In partial fulfillment of the requirements for the award of the Degree of

MASTER OF PHARMACY

IN

BRANCH- I - PHARMACEUTICS

Submitted by

R. SAPTHASRI

REGISTRATION No: 261910159

Under the guidance of

Mrs. M.A AMUTHA GNANA ARASI, M. Pharm., Ph.D.,

Department of Pharmaceutics

COLLEGE OF PHARMACY

SRI RAMAKRISHNA INSTITUTE OF PARAMEDICAL SCIENCES

COIMBATORE – 641044

October-2021

Certificates

CERTIFICATE

This is to certify that the M. Pharm dissertation entitled **"SILYMARIN LOADED SUPER PARAMAGNETIC IRON OXIDE NANOPARTICLE (SPIONS) FOR TARGETING SARS COV-2 TO COMBAT COVID-19"** being submitted to The Tamil Nadu Dr. M.G.R. Medical University, Chennai was carried out by **R. SAPTHASRI (Register no: 261910159)** in the Department of Pharmaceutics, College of Pharmacy, Sri Ramakrishna Institute of Paramedical Sciences, Coimbatore, under my direct supervision, guidance and to my fullest satisfaction.

Mrs. M. A. AMUTHA GNANA ARASI, M. Pharm., Ph.D.,
Assistant Professor,
Department of Pharmaceutics,
College of Pharmacy,
SRIPMS,
Coimbatore – 641 044.

Place: Coimbatore
Date:

CERTIFICATE

This is to certify that the M. Pharm dissertation entitled **"SILYMARIN LOADED SUPER PARAMAGNETIC IRON OXIDE NANOPARTICLE (SPIONS) FOR TARGETING SARS COV-2 TO COMBAT COVID-19"** being submitted to The Tamil Nadu Dr. M.G.R. Medical University, Chennai was carried out by **R. SAPTHASRI (Register no: 261910159)** in the Department of Pharmaceutics, College of Pharmacy, Sri Ramakrishna Institute of Paramedical Sciences, Coimbatore, under the direct supervision and guidance of **Dr. M.A. AMUTHA GNANA ARASI, M. Pharm., Ph. D.,** Assistant Professor, Department of Pharmaceutics, College of Pharmacy, Sri Ramakrishna Institute of Paramedical Sciences, Coimbatore.

Dr. M. GOPAL RAO, M. Pharm, Ph.D.,
Vice Principal & HOD,
Department of Pharmaceutics,
College of Pharmacy,
SRIPMS,
Coimbatore - 641 044.

Place: Coimbatore
Date:

CERTIFICATE

This is to certify that the M. Pharm dissertation entitled **"SILYMARIN LOADED SUPER PARAMAGNETIC IRON OXIDE NANOPARTICLE (SPIONS) FOR TARGETING SARS COV-2 TO COMBAT COVID-19"** being submitted to The Tamil Nadu Dr. M.G.R. Medical University, Chennai was carried out by **R. SAPTHASRI (Register no: 261910159)** in the Department of Pharmaceutics, College of Pharmacy, Sri Ramakrishna Institute of Paramedical Sciences, Coimbatore, under the direct supervision and guidance of **Dr. M.A AMUTHA GNANA ARASI, M.Pharm., Ph. D.,** Assistant Professor, Department of Pharmaceutics, College of Pharmacy, Sri Ramakrishna Institute of Paramedical Sciences, Coimbatore.

Dr. T.K. RAVI, M. Pharm, Ph.D., FAGE.
Principal,
College of Pharmacy,
SRIPMS
Coimbatore -641 044.

Place: Coimbatore
Date:

Acknowledgement

ACKNOWLEDGEMENT

I thank **God Almighty** for the wisdom and perseverance that had been bestowed upon me during this research project. It's because of His grace I was able to successfully complete my project even though under going all the hurdles and suffering.

I would like to express my gratitude and respect towards my guide, **Mrs. M.A. Amutha Gnana Arasi, M. Pharm., Ph. D.,** Assistant Professor, Department of Pharmaceutics, who mentored me in this pharmaceutical research work.

My sincere gratitude to our beloved Principal **Dr. T.K.Ravi**, **M.Pharm., Ph.D., FAGE.,** for supporting and providing every need from time to time to complete this work successfully.

I express my deep sense of gratitude and indebtedness to **Dr. M. Gopal Rao, M.Pharm., Ph.D.,** Vice principal and Head, Department of Pharmaceutics, for his valuable suggestions and support during this project.

I submit my sincere thanks to our beloved Managing Trustee **Thiru. R. Vijayakumhar, Managing Trustee, M/s. SNR Sons Charitable Trust**, Coimbatore for providing all the facilities to carry out this work.

I owe my profound gratitude to **Dr. M. Gandhimathi, M.Pharm., Ph.D.,** for helping me to carry out the analytical studies and also for being a beacon of wisdom in resolving any challenges I faced during the course of work.

My sincere thanks to my dear teachers **Dr. S. Krishnan M.Pharm., Ph.D., Dr. K. Muthuswamy, M.Pharm., Ph.D., Dr. J. Bhagyalakshmi, M. Pharm., Ph.D., Dr. A.S. Manjuladevi M.Pharm., Ph.D., and Dr. R.M. Akila M.Pharm., Ph.D.** for their moral support and guidance during the course of work.

I would also like to thank **Dr. Venkataswamy, M.Sc., Ph.D., Mr.S. Muruganandham, and Mrs. vishala** for their kind co-operation during this work.

I remain greatly indebted to my parents **Mr. R. D Ravichandran and Mrs.k. Lashmi** and my brothers **Mr. Jeevanand and Mr. krishva** for their precious love, affection and moral support which kept me on high spirits and are also the backbone for all successful endeavors in my life.

Words cannot express my gratitude to my friends **S. Agneeshwaran, R. Aravind Raj, Y. Arul Packiadhas, C. Bavya, P. Hari, M. Janani, Navaneeth Krishnan, M.K Nithin, Sweety Joen, S. Shanmuga Priya, Midhuna, Bharma sundari, Keerthi, Shali Shaji, Thiyal Nayaki, Banupriya and M. Dhinesh** for their support, cooperation and inspiration during the course of my work.

I wish to extend my sincere thanks to all my batchmates, seniors and juniors who directly or indirectly helped me during my work.

I express my gratitude to all my dear teachers, friends and relatives for their support during my work.

R. Sapthasri

Abbreviations

LIST OF ABBREVIATION

1. SARS-COV 2 - Severe Acute Respiratory Syndrome Coronavirus -2
2. RNA - Ribonucleic acid
3. HIV - Human Immunodeficiency Virus
4. SPIONS - Super Paramagnetic Iron Oxide Nanoparticles
5. UV -VIS - Ultraviolet – Visible
6. EC - Ethyl Cellulose
7. PEG - Poly Ethylene Glycol
8. SEM - Scanning Electron Microscopy
9. FTIR - Fourier Transform Infrared Spectroscopy
10. 5N11 - Human beta1-coronavirus (β1CoV) OC43
11. 7MJP - SARS-CoV-2 receptor binding domain in complex with neutralizing antibody COVA2-39)
12. 7JMO - SARS-CoV-2 receptor binding domain in complex with neutralizing antibody COVA2-04)
13. 4RNA - Middle East Respiratory Syndrome (MERS) coronavirus
14. 6VYB - SARS-CoV-2 spike ectodomain structure
15. 6LU7 - COVID-19 main protease in complex with an inhibitor N3
16. 7LMF - SARS-CoV-2 3CLPro in complex with 2-(benzotriazol-1-yl)-N-[4-(1H-imidazol-4-yl)phenyl]-N- (3-thienylmethyl)acetamide
17. 6VXX - SARS-CoV-2 spike glycoprotein
18. 7LMF - SARS-CoV-2 3CLPro in complex with 2-(benzotriazol-1-yl)-N-[4-(1H-imidazol-4-yl)phenyl]-N-(3-thienylmethyl)acetamide
19. GLN - Glutamine
20. LYS - Lysine
21. PRO - Proline
22. PHE - Phenylalanine
23. ASN - Asparagine
24. GLU - Glutamic acid
25. TYR - Tyrosine
26. GLN - Glutamine
27. VAL - Valine
28. LEU - Leucine
29. HIS - Histidine
30. ILE - Isoleucine
31. TRP - Tryptophan
32. LYS - Lysine
33. ALA - Alanine
34. TRP - Tryptophan
35. ASP - Aspartic acid
36. GLY - Glycine
37. PHE - Phenylalanine
38. ASN - Asparagine
39. MET - Methionine
40. THR - Threonine

List of Tables

LIST OF TABLES

List of Figures

LIST OF FIGURES

Contents

CONTENTS

Introduction

INTRODUCTION

A novel coronavirus causing pneumonia was identified in China in December 2019. On February 11, the Coronavirus Study Group (CGS) of the International Committee on Virus Taxonomy (ICTV) designated the virus as SARS-CoV-2 based on phylogeny and taxonomy. The same day, the Director General of the World Health Organization (WHO) designated the disease caused by SARS-CoV-2 "coronavirus disease 2019" (COVID-19). On March 11, 2020, the WHO declared the COVID-19 outbreak a pandemic. As of May 2020, SARS-CoV-2 has spread across the world in over 185 countries, with millions of infections and hundreds of thousands of deaths[1].

SARS-CoV-2 belongs to Coronaviridae family such as SARS-CoV, MERS-CoV and SARS-CoV-2 are enveloped viruses with a positive single-stranded RNA genome. SARS-CoV-2 viral particles are spherical to pleomorphic and 65 to 125 nm in size. Inside the particle, the viral RNA, with 29,811 nucleotides, is tightly coiled and coated by the nucleocapsid (N) protein. Three glycoproteins, called spike (S), membrane (M), and envelope (E), are embedded in the lipid outer membrane. Spike proteins form homotrimers, which protrude from the lipid envelope and form the characteristic "corona". Spike proteins mediate viral entry into host cells by binding to angiotensin-converting enzyme 2 (ACE2) expressed on respiratory tract cells[2].

Currently, COVID-19 has non-specific treatment. In humans, COVID-19 kicks off the respiratory system through droplets from coughs and sneezes of infected persons. Generally, respiratory system can be divided into two regions namely upper (nasal cavity, sinuses, nasopharynx, oropharynx, larynx, and trachea) and lower tract (bronchioles, alveolar ducts and alveolar sacs). Their journey to the lower respiratory tract after infecting the upper respiratory tract is the cause of respiratory illness[1].

Major obstacles in drug delivery to upper respiratory tract are smaller surface area, lower blood flow, mucus layer (traps inhaled substances) and filtration of foreign objects. The large surface area, ciliated cells of lower respiratory tract may be ideal area for delivery as it is connected directly to systemic circulation via pulmonary circulation with few challenges like branched nature alveolar macrophages and pulmonary surfactant (phospholipids, proteins and mucins) decrease delivery efficiencies. However, the delivery to lower tract should overcome muco-ciliary and cough clearance mechanisms.

The current treatments are mainly based on symptomatic relief and respiratory support in seriously ill patients. Most of the currently available drugs for the treatment of viral infections fall in one of the followings classes: antiviral therapies, immune therapy, anti-inflammatory therapy, and other treatments that include traditional medicines based on natural products[3]. RNA-dependent RNA polymerase (RdRp) and Angiotensin-converting enzyme 2 (ACE2) are also viable drug targets for COVID-19 treatment. Some antiviral drugs like Favinavir, Ritonavir, Oseltamivir, Lopinavir, Ganciclovir and Remdesivir are clinically tested against COVID-19 infection.

The development of new drugs is lagging because of the long process necessary to prove their efficacy and safety. To overcome these limitations and to improve antiviral treatments, multidisciplinary research efforts are required toward the development of alternative antiviral therapies, targeting different phases in the viral replication cycle. In this regard, nanotechnology has attracted increasing attention and has already been investigated for potential use in the prevention and/or treatment of viral infection[4].

Nanotechnology is a rapidly growing field with potential applications in health and drug therapy due to their small size, large surface area, in vivo drug delivery characteristics, and unusual electronic optical, and magnetic properties. Upon decreasing the particle size (to less than 100 nm), the number of atoms on the surface is greater than that inside the particle, thus meaning that these particles can give better results than, and frequently have different biological activity to, their chemical components[5].

Nanotechnology offers a number of solutions to fight viruses, both outside and inside the host, and several nanotechnologybased platforms have already been successful in preclinical studies to counter several human viral pathogens such as HIV, human papilloma virus, herpes simplex, and respiratory viruses.

Nanotechnology-based approaches should be leveraged to help the fight against COVID-19 as well as any future pandemics, in a number of ways, including

(i) novel vaccines and drugs, where nanomaterials can be leveraged for direct delivery of broad-spectrum antivirals and to support targeted therapies to the lungs;
(ii) highly specific, rapid, and sensitive tests to detect infection or to detect immunity (serological tests);
(iii) superfine filters for face masks or blood filtering;

(iv) novel surfaces or surface coatings that are resistant to viral adhesion and can inactivate the virus; and

(v) the improvement of tools for contact tracing[4].

Superparamagnetic iron oxide nanoparticles (SPIONs)

Magnetic nanoparticles (MNPs) exhibit para magnetism in the absence of external magnetic field. However, MNPs display super-para magnetism in the presence of magnetic field. The particles such as meghemite/megnitite (chemical formula: -Fe_2O_3 repeating units) contain exceptional optical, electrical and chemical properties which permit their applications in virus detection, magnetic cell separation, enzyme catalysis, gene therapy, targeting chemotherapy, radiotherapy, diagnostics, therapeutics, bio-sensing and information storage. Magnetic nanoparticles exhibiting such properties offer vast advantages over traditional macro or microparticles in targeted drug delivery and treatment[6].

In various clinical studies, these particles have shown the capabilities of deep-tissue imaging, low toxicity and non-immunogenicity. This is due to their high magnetic responsiveness, biodegradability, biocompatibility, high delivery efficiency and potential targeting function. Moreover, iron oxide nanoparticles are the only magnetic nanoparticles approved for clinical application by the US Food and Drug Administration (FDA).

In a number of studies, Super Paramagnetic Iron Oxide Nanoparticles (SPIONs) have been used for diagnostic and therapeutic applications such as magnetic resonance imaging (MRI) by contrast agents, magnetic hyperthermia in cancer treatment and radio sensitization in radiotherapy. In addition, drugs can be loaded onto magnetic nanoparticles for targeted therapy with the aid of an external magnet. For this purpose, magnetic Fe3O4 nanoparticles are firstly prepared and then are encapsulated in copolymers[7].

Synthesis of SPIONs

The basic strategies involved in the formation of SPIONs are physical, wet chemical, and microbial methods. Each method has its own advantages and disadvantages, and impacts over various properties of SPIONs. In this section, the predominant chemical procedures used for synthesizing SPIONs have been reviewed with typical examples[8].

Co-precipitation method

Co-precipitation method is the widely used technique for synthesizing black and/or brownish SPIONs by precipitating an aqueous solution mixture containing ferric and ferrous salts (in a 2:1 stoichiometric ratio) using a base, at room or elevated temperatures (70–90◦C), in the absence of oxygen[9]. The co-precipitation process occur through either one of the two topotactic phase transformation pathways (i) akageneite phase (birth of crystal nuclei) to goethite phase (to form arrow-shaped nanoparticles) or (ii) ferrous hydroxide phase to lepidocrocite phase to finally form SPIONs, depending upon the slow (for example, 1.88 ml/min) or quick (at once) addition of base into the mixture of precursor solution[10].

The above transformations include hydroxylation and condensation (either through olation or oxolation mechanisms) of Fe3+ and Fe2+ ions based on the pH of the colloidal solution. Moreover, surfactants/capping agents are used to control the growth of SPIONs during the synthesis. However, the magnetic properties of SPIONs are significantly influenced by synthesis parameters such as reaction timings, base molarity, stirring rate, and the type of base. Recently, Vikram et al. (2014)[10] showed that the stoichiometric ratio of Fe2+ and Fe3+ and the base addition rate also have control over the regulation of the magnetic properties of SPIONs. They reported that the change in concentration of the base yielded nanomaterials with ferromagnetic behavior instead of super Para magnetism.

The main drawback of this co-precipitation method is the lack of proper crystallinity and broad particle size distribution which leads to low saturation magnetization value (30–50 emu/g) of the SPIONs as compared to the bulk magnetization value of Fe3O4 nanoparticles (92 emu/g). Nevertheless, magnetic nanoparticles with uniform size of 9 nm were obtained via co-precipitation method using a tetramethylammonium hydroxide for MRI contrast[11].

Thermal decomposition method

Highly crystalline and monodisperse SPIONs with diverse sizes and shapes can be synthesized via thermal decomposition method in the presence of surfactants (for example, oleic acid and oleylamine and organic solvents with high boiling points. Solvent free thermal decomposition of iron precursors can also be utilized for preparing magnetic nanoparticles[12].

However, the resulting hydrophobic SPIONs tend to show good dispersibility only in organic solvents (for example, tetrahydrofuran) because of their hydrophobic interactions between

surfactants and solvents. Many synthesis parameters such as concentration of surfactants, reaction temperatures, reaction timings, ratio of precursors to surfactants, solvents and heating rate during reflux govern the physicochemical characteristics and magnetic properties of SPIONs[13].

The hydrophobic SPIONs are converted to water soluble ones by using either ligand exchange method or bilayer surfactant stabilization method to involve them instantaneously into cancer theranostic applications. For example, Xu et al. (2008)[14] replaced the hydrophobic surface coatings formed of oleate and oleyl amine molecules with a hydrophilic coating of dopamine attached PEG through ligand exchange method, since dopamine tended to show more affinity to attach with the surface of iron oxide nanoparticles as compared to the hydrophobic coatings. In the bilayer surfactant stabilization, the bilayers are formed by the insertion of hydrophobic part of an amphiphilic molecule in between the long hydrophobic chains of surfactants whose end functional groups, for instance carboxyl groups, are attached to the surface atoms of magnetic nanoparticles. Recently, oleic acid was used to form bilayers on the surface of magnetic nanoparticles after optimizing their concentration with respect to the formed nanoparticles[15]. But, these conversion methods are tedious and seriously affect the magnetic properties, colloidal dispensability and yield of SPIONs[16]. To overcome these problems, hydrophilic SPIONs can be directly synthesized by one-pot thermolysis method using polyol-based surfactants and/or solvents[11].

Hydrothermal method

In hydrothermal method, the precursors are dissolved in an aqueous solution along with surfactants/capping agents, and sealed in a Teflon coated autoclave, where high temperature and high pressure are maintained to synthesize SPIONs with definite sizes and shapes. Finally, the temperature of the autoclave is allowed to cool down to room temperature and the resultant supernatant solution is washed to remove unused surfactants/capping agents, impurities and unreacted precursors. The parameters such as heating temperatures, reaction timings and the ratio of the precursor to surface coatings are manipulated to obtain biocompatible SPIONs with various sizes, shapes and magnetic properties for MRI contrast and cancer hyperthermia. In a study, ethylene glycol played an important role in synthesizing SPIONs with three different morphologies (polyhedron/rod shaped, porous sphere and flowerlike) with saturation magnetization 66–73.5 emu/g, in which flowerlike nanoparticles possessed the lowest magnetization (66 emu/g) ascribed to the shape and size induced magnetic

properties reduction[17].Nonetheless, this method has disadvantages such as producing moderately crystalline SPIONs as compared to magnetic nanoparticles synthesized via thermolysis method[18] and consuming more time.

Microemulsion method

Two immiscible phases (oil and water) are used to form SPIONs under the presence of stabilizing agents by forming a monolayer at the interface between the immiscible phases. Water-in-Oil (W/O) and Oil-in-Water (O/W) are the two kinds of microemulsions formed to synthesize different kinds of nanoparticles. The hydrophilic and hydrophobic parts of surface coatings play a major role in (i) stabilizing nanoparticles, (ii) catering chemical reactions to happen and (iii) controlling physicochemical parameters. W/O microemulsion method is frequently used to form SPIONs, where the stabilizing agents in continuous oil phase initially protect the droplets formed of iron oxide reactants, which then react to form SPIONs. The sizes and shapes are controllable by varying the concentrations of iron oxide precursor to base, surfactant and/or solvents. Recently, cetyl trimethylammonium bromide (CTAB)[19] and synperonic 10/6[20] were used to tailor the size of the SPIONs. Similarly, SPIONs with different sizes (6.5, 4.2 and 8.7 nm) were synthesized by varying the ratio of concentrations of iron oxide precursor to base (1:1 and 2:1)[21]. Nevertheless, the removal of unreacted precursors, base and surfactants is intricate in this microemulsion method.

Sonochemical method

Sound energy such as ultrasound can be used for synthesizing SPIONs, where the cavitation bubbles produced by such ultrasound transform the reactants into desired products at ambient temperatures. The size and shapes of SPIONs can be varied by controlling the refluxing time, irradiation time and power. Recently, Dolores et al. (2015)[22] reported that production of Fe3+ ions for making iron oxide nanoparticles (using ethylene glycol as surfactant) increased in a linear fashion with the increase in reaction time at a particular ultrasonic frequency (581 kHz) as compared to other frequencies (861 and 1141 kHz).

Microwave-assisted synthesis

Microwave energy can also be utilized for synthesizing SPIONs in a very short period of time at low energy consumption. A uniform heat is provided by microwaves inside the reaction containers from all sides for synthesizing stable and high crystalline iron oxide

nanoparticles. But these nanoparticles have reduced surface reactivity (due to the low energy surface crystalline facets), which is assessed based on their interaction with water and aggregate formation process[23]. Interestingly, the low surface reactive nanoparticles can enhance the stability of SPIONs[24], which is an advantage of this method. The magnetic properties of SPIONs can be controlled by manipulating the concentration of surfactants.

Considerations in design of magnet-based carriers

A magnetically-driven delivery system uses SPION as carriers to facilitate fast extracellular, intracellular, and site-specific/targeted delivery of biotherapeutics under the influence of an external magnetic field. As administered SPIONs can be stacked up in the area with strong magnetic field upon application of an external magnet. In this way, biotherapeutics coated on or mixed with SPIONs can be guided to localize and be retained in specific tissue or organ sites. This may improve target specificity and therapeutic efficacy. An external magnetic field can also accelerate cellular uptake of nanoparticles in 2D and 3D culture systems *invitro.*

Magnetic fields are safe and are widely used in clinics.in vivo safety of magnetic field of > 10 tesla is to be demonstrated. Magnetically-driven accumulation of SPIONs can be a promising treatment for localized disease. For successful delivery of biotherapeutics using magnetic carriers, several criteria should be maintained. First, magnetic carriers should be stable and remain constant in size and magnetic property during the course of treatment. Second, magnetization of the SPION-based carrier must be sufficient in response to the applied magnetic field. At the same time, exterior magnetic fields in terms of magnetic flux density and permeability should be optimized to be strong enough to mediate penetration of biotherapeutics across the biological barriers and sufficient accumulation at target sites while remaining safe to normal tissue. Proper formulation of SPION using diverse materials like polymers and lipids not only increases the rate of response to external magnetic fields and the yield of accumulation/retention of biotherapeutics at target sites, but also enables simultaneous delivery of multiple drugs and functional agents incorporated in one carrier[25].

SILYMARIN

Silymarin, a potential phytochemical compound obtained from the seeds of Silybum marianum (milk thistle) plant has been used as a hepatoprotective agent for more than a decade. Silymarin shows strong anti-oxidant effect through scavenging free radicals and inhibiting peroxidation of lipids. The drug is well tolerated and has relatively few adverse effects. The

effectiveness of silymarin as hepatoprotective agent was diminished by its poor water solubility and low bioavailability. The poor bioavailability is mainly due to extensive metabolism, poor aqueous solubility and rapid excretion through urine and bile, and low permeability across intestinal epithelial cells. Besides silymarin has been extensively studied in vitro and in vivo for its cancer chemo preventive potential against various cancers.

The oral bioavailability of silibinin, however, is extremely low (b1%) caused primarily by its poor gut absorption and phase II metabolism in the liver. It was determined that gut permeability was not the rate-limiting step in the gut absorption of silibinin; instead it was the slow dissolution rate of silibinin due to its poor solubility in the gastrointestinal fluid. The high incidence of administration of silymarin together with its short half-life and poor bioavailability proposed great scope for the proposal and development of nanoparticulate drug delivery systems.

Silymarin has been studied for treatment of acetaminophen overdose injuries of the liver, kidney problems, improper working of cerebral cortex, histological changes and antioxidant activity. It has been also reported to reduce the effects of Aflatoxin B1 in bovine calves. Silymarin has been used for the reduction glycemic level and progression of the complications related to diabetes which has been reported to enhances the rate of cardiovascular disease and kidney problems in Europe and United States

Silymarin as Antiviral Agents

The primary bioactive components of the extract consist of several flavonolignans (silybin, silychristin, silydianin, isosilybin, and dehydrosilybin), and a few flavonoids, mainly taxifolin. The mixture of silybin A and silybin B (1:1) is also known as silibinin ($C_{25}H_{22}O_{10}$), which makes up the major active ingredient (roughly 50%) of silymarin. Now evidence suggests that the extract possesses potent antiviral activities against numerous viruses, particularly hepatitis C virus (HCV). Consequently, silymarin is the most commonly consumed herbal product among HCV-infected patients in western countries. Antiviral efficacy of silymarin has also been reported against human papillomavirus, a highly carcinogenic virus[26].

Various antiviral activities of silymarin and derivatives have been shown against liver and non-liver pathogens, making them potential broad-spectrum antivirals, for some of the enveloped viruses explored to date. In addition, considering the poly pharmacological activity of silymarin and derivatives towards multiple host cell targets, such as cell innate immunity

and inflammation, oxidative stress production, and autophagy, which are all cell physiological processes that are known to be elicited or subverted by many viral infections, these natural products are likely to exert their antiviral activities by modulating the cellular environment in addition to any potential direct antiviral function(s) against a specific viral protein[27].

Recent studies documented the antiviral activities of Silymarin against several viruses; including flaviviruses (hepatitis C virus and dengue virus), togaviruses (Chikungunia virus and Mayaro virus), influenza virus, hepatitis B virus and Human Immunodeficiency Virus (HIV); in addition to its anti-oxidative and anti-inflammatory role. Furthermore, a recent study demonstrated the role of Silymarin in attenuating cigarette smoke extract-induced inflammation via simultaneous inhibition of autophagy and extracellular signal-regulated kinase/p38 mitogen-activated protein kinase (ERK/ p38 MAPK) pathway in human bronchial epithelial cells, as well as attenuating up-regulation of pro-inflammatory cytokines TNF-α, IL-6 and IL-8 and concluded that Silymarin might be an ideal agent treating inflammatory pulmonary disease. This clinical trial aim was evaluating the role of Silymarin in the treatment of adults with COVID-19 Pneumonia[28].

Literature Review

LITERATURE REVIEW

Das *et.al,* (2011) synthesised Silymarin nanoparticles by nanoprecipitation in polyvinyl alcohol stabilized Eudragit polymer. Silymarin is a polyphenolic component extracted from Silybum marianum. It is an antioxidant, traditionally used as an immunostimulant, hepatoprotectant, and dietary supplement. Silymarin has proved to be a valuable chemo preventive and a useful antineoplastic agent. Medical success for Silymarin is, however, constrained by very low aqueous solubility and associated biopharmaceutical limitations. Silymarin flavonolignans are also susceptible to ion-catalysed degradation in the gut. Proven antihepatotoxic activity of Silymarin cannot therefore be fully exploited in acute chemical poisoning conditions like that in paracetamol overdose. Moreover, a synchronous delivery that is required for hepatic regeneration is difficult to achieve by itself. This work is meant to circumvent the inherent limitations of Silymarin through the use of nanotechnology. Process parameter optimization provided 67.39% entrapment efficiency and a Gaussian particle distribution of average size 120.37 nm. Silymarin release from the nanoparticles was considerably sustained for all formulations. Silymarin were strongly protective against hepatic damage when tested in a paracetamol overdose hepatotoxicity model. Nanoparticles recorded no animal death even when administered after an established paracetamol-induced hepatic necrosis. Preventing progress of paracetamol hepatic damage was traced for an efficient glutathione regeneration to a level of 11.3 µmol/g in hepatic tissue due to Silymarin [49].

Prados *et.al,* (2012) overviewed doxorubicin nanoplatform-based delivery systems and the principal advances obtained in breast cancer chemotherapy. Doxorubicin, one of the most effective anticancer drugs currently known, is commonly used against breast cancer. Nanotechnology is a promising alternative to overcome these limitations in cancer therapy as it has been shown to reduce the systemic side-effects and increase the therapeutic effectiveness of drugs. Furthermore, the wide range of nanoparticle systems available may provide a solution to the different problems encountered during doxorubicin-based breast cancer treatment. Thus, a suitable nanoparticle system may transport active drugs to cancer cells using the pathophysiology of tumours, especially their enhanced permeability and retention effects, and the tumour microenvironment. In addition, active targeting strategies may allow doxorubicin to reach cancer cells using ligands or antibodies against selected tumour targets. Similarly, doxorubicin resistance may be overcome, or at least reduced, using nanoparticles that are not recognized by P-glycoprotein, one of the main mediators of multidrug resistance, thereby

resulting in an increased intracellular concentration of drugs. This paper provides an overview of doxorubicin nanoplatform-based delivery systems and the principal advances obtained in breast cancer chemotherapy[5].

Yang *et.al,* (2012) reviewed Potential of magnetic nanoparticles for targeted drug delivery. Nontoxic superparamagnetic magnetic NPs (MNPs) with functionalized surface coatings can conjugate chemotherapeutic drugs or be used to target ligands proteins, making them useful for drug delivery, targeted therapy, magnetic resonance imaging, transfection, and cell protein DNA separation. To optimize the therapeutic efficacy of MNPs for a specific application, three issues have been addressed. First, the efficacy of magnetic targeting guidance is dependent on particle magnetization, which can be controlled by adjusting the reaction conditions during synthesis. Second, the tendency of MNPs to aggregate limits their therapeutic use *in vivo* surface modifications to produce high positive or negative charges can reduce this tendency. Finally, the surface of MNPs can be coated with drugs which can be rapidly released after injection, resulting in targeting of low doses of the drug. Drugs therefore need to be conjugated to MNPs such that their release is delayed and their thermal stability enhanced. The author describes the creation of nanocarriers with a high drug-loading capacity comprised of a high-magnetization MNP core and a shell of aqueous, stable, conducting polyaniline derivatives and their applications in cancer therapy[39].

Hsu *et.al,* (2012) studied the nanoprecipitation technique to develop a nanoparticles system to improve the solubility of silymarin. The newly developed silymarin nanoparticles were characterized for mean particle size, morphology, intermolecular interaction, crystalline features and dissolution property, as well as assessing for antioxidant activities. Silymarin, a well known hepatoprotective drug, has been routinely used in treating liver disorders. However, its bioavailability and therapeutic efficiency are limited by the poor aqueous solubility. Results has been indicated that a drastic change in the physiochemical properties of silymarin was noted in the form of nanoparticles, as displayed by the extremely small particle size (46.1 +/- 1.73 nm), the formation of intermolecular hydrogen bonding between silymarin and matrix of nanoparticles, and the rendering of amorphous state. These phenomena have contributed to the enhanced dissolution property of silymarin nanoparticles, as well as a greater potency in DPPH radical scavenging, anti-superoxide anion formation, and superoxide anion scavenging activities than the crude silymarin. This study concludes that silymarin nanoparticles have an improved physicochemical property as demonstrated by an increased solubility and enhanced antioxidant activities[47].

Okoli *et.al,* (2012) formulated magnetic iron oxide nanoparticles and further performed Comparison and functionalization study of microemulsion. Magnetic iron oxide nanoparticles (MION) for protein binding and separation were obtained from water-in-oil (w/o) and oil-in-water (o/w) microemulsions. Characterization of the prepared nanoparticles have been performed by TEM, XRD, SQUID magnetometry, and BET. Microemulsion-prepared magnetic iron oxide nanoparticles (ME-MION) with sizes ranging from 2 to 10 nm were obtained. Study on the magnetic properties at 300 K shows a large increase of the magnetization ~35 emu/g for w/o-ME-MION with superparamagnetic behavior and nanoscale dimensions in comparison with o/w-ME-MION (10 emu/g) due to larger particle size and anisotropic property. Moringa oleifera coagulation protein (MOCP) bound w/o- and o/w-ME-MION showed an enhanced performance in terms of coagulation activity. A significant interaction between the magnetic nanoparticles and the protein can be described by changes in fluorescence emission spectra. Adsorbed protein from MOCP is still retaining its functionality even after binding to the nanoparticles, thus implying the extension of this technique for various applications[20].

Raj *et.al,* (2013) developed and evaluated naturally obtained polysaccharides (Tamarind seed polysaccharide and Pectin) as a carrier in colon targeted drug delivery systems a colon targeted drug delivery. The newer developments in this context aim for an increased selectivity of drug delivery by targeting mechanisms which have a closer relation to pathophysiological particularities of the disease. The polysaccharides were characterized of its physical properties. The interaction between the excipients and prednisolone was also studied through FTIR spectroscopy. Tablets were then prepared by wet granulation method with different ratio of polysaccharides and evaluated for their physical properties like weight variation, hardness, friability and content uniformity. In vitro drug release studies were performed in conditions simulating stomach to colon transit. No significant release was observed at acidic pH, however, when it reached the colonic pH where, drug release was observed. Also, release of drug was found to be higher in presence of rat caecal content. Data were fitted to various kinetic models. The mechanism of drug release from tablets was found to be non-Fickian, anomalous transport[37].

Hyejung Mok and Miqin Zhang (2013) reviewed the recent advances in use of SPION-based carrier systems to improve the delivery efficiency and target specificity of biotherapeutics. The examination of various formulations of SPION-based delivery systems, including SPION micelles, clusters, hydrogels, liposomes, and micro/nanospheres, as well as

their specific applications in delivery of biotherapeutics. Superparamagnetic iron oxide nanoparticle (SPION)-based carrier systems have many advantages over other nanoparticle-based systems. They are biocompatible, biodegradable, facilely tunable, and superparamagnetic and thus controllable by an external magnetic field. These attributes enable their broad biomedical applications. In particular, magnetically-driven carriers are drawing considerable interest as an emerging therapeutic delivery system because of their superior delivery efficiency. Recently, biotherapeutics including therapeutic cells, proteins and genes have been studied as alternative treatments to various diseases. Despite the advantages of high target specificity and low adverse effects, clinical translation of biotherapeutics has been hindered by the poor stability and low delivery efficiency compared to chemical drugs. Accordingly, biotherapeutic delivery systems that can overcome these limitations are actively pursued. SPION-based materials can be ideal candidates for developing such delivery systems because of their excellent biocompatibility and superparamagnetism that enables long-term accumulation/retention at target sites by utilization of a suitable magnet. In addition, synthesis technologies for production of finely-tuned, homogeneous SPIONs have been well developed, which may promise their rapid clinical translation[51].

Gupta et.al, (2014) investigated to enhance the hepatoprotective activity of silymarin by incorporating it in chitosan (Ch) nanoparticles (NPs) for passive targeted delivery, thereby prolonging its retention time. Silymarin loaded nanoparticle were prepared by ionic gelation technique, which were then optimized using a central composite design in order to minimize the particle size and maximize the drug entrapment efficiency. The optimized formulation was evaluated for in vitro drug release study and in vitro study on Swiss Albino mice using carbon tetrachloride (CCL4) induced hepatotoxicity model. In vitro dissolution studies illustrated sustained, zero order drug release from optimized formulation and also its therapeutic potential was amplified during in vitro studies on Swiss Albino mice using CCL4 induced hepatotoxicity model. The results suggested that NPs of silymarin could successfully enhance its hepatoprotective effect by passive targeting and sustained release[44].

Muhammad *et.al,* (2014) analyzed the inhibitory action of quercetin glycosides by computational docking studies. For this, natural metabolite quercetin glycosides isolated from buckwheat and onions were used as ligand for molecular interaction. The crystallographic structure of molecular target angiotensin-converting enzyme (ACE) (peptidyl-dipeptidase A) was obtained from PDB database (PDB ID: 1O86). Enalapril, a well-known brand of ACE inhibitor was taken as the standard for comparative analysis. Computational docking analysis

was performed using PyRx, AutoDock Vina option based on scoring functions. The quercetin showed optimum binding affinity with a molecular target (angiotensin-converting-enzyme) with the binding energy of −8.5 kcal/mol as compared to the standard (−7.0 kcal/mol). These results indicated that quercetin glycosides could be one of the potential ligands to treat hypertension, myocardial infarction, and congestive heart failure[46].

Khalkhali *et.al.*, (2015) prepared and characterized magnetic nanoparticles (MNPs) as theranostic system to act simultaneously as drug carrier and MRI contrast agent. Chitosan-coated MNPs (CMNPs) were prepared and loaded with silymarin by co-precipitation method. Chitosan was selected to provide steric stabilization around MNPs and provide stable aqueous dispersion. Silymarin-loaded CMNPs were characterized with various techniques and their potential as MRI contrast agent was also evaluated. Particle size analysis (DLS) and scanning electron microscopy (SEM) confirmed the formation of spherical nanoparticles with the final average particle size about 18 nm. The Vibrating Sample Magnetometer (VSM) analysis demonstrated the saturation magnetization values of 29.08 emu/g for CMNPs. Entrapment efficiency and drug loading for silymarin were calculated to be 95 and 10%, respectively. The finding revealed that CMNPs provide a sustained release pattern. It was found that the maximum drug release accessible for CMNPs in pH 5.3 was higher than pH 7.4 [30].

Kouchakzadeh *et.al,* (2015) has studied the production of human serum albumin (HSA) nanoparticles using desolvation technique that were simultaneous loaded with high amounts of superparamagnetic iron oxide nanoparticles (SPIONs) and 5-flourouracil (5-FU) was investigated on utilizing biocompatible magnetic nanoparticles (MNPs) for biomedical applications. The optimum conditions found to be pH of 8.2, drug concentration of 1.5 mg/ml and SPIONs concentration of 2.79 mg/ml. Under the mentioned optimum conditions, particles with the size of 111.8 nm, zeta potential of -37.1 mV, 5-FU loading of 15.8% and SPIONs entrapment efficiency of 41.1% were obtained[33].

Tewes *et.al,* (2015) formulate and evaluate the aerodynamic properties of SPIONs-loaded Trojan microparticles after delivery from a dry powder inhaler. It was potentially achieved with porous microparticles PEG and hydroxypropyl-β-cyclodextrin loaded with superparamagnetic iron oxide nanoparticles (SPIONs) in combination with a target-directed magnetic gradient field to the lung to improve therapeutic efficiency and minimise unwanted side effects. Trojan particles appeared highly sensitive to the magnetic field and their deposition on most of the stages of the next generation cascade impactor (NGI) was changed in the presence compared to the absence of the magnet. If loaded with a pharmaceutical active ingredient, these particles

may be useful for treating localized lung disease such as cancer nodules or bacterial infectious foci[34].

Khan *et.al,* (2015) reviewed on the properties of magnetic nanoparticles (MNPs), various approaches for their synthesis, and their biomedical applications. First part of this review focuses on the classes, physical properties, and characteristics of MNPs. The second part sheds light on strategies developed for the synthesis of MNPs, with special attention given to biological, physical, and chemical approaches as well as recent modifications in the preparation of monodispersed samples. Furthermore, this review deals with the biomedical applications of MNPs, which includes applications in targeted drug delivery, diagnostics, gene therapy, hyperthermia and advantages in the field of medicine[6].

Liu *et.al,* (2016) prepared highly bioavailable silibinin nanoparticles using nano emulsification technique and were physicochemically characterised as silibinin have poor solubility and bioavailability, restricting its clinical use. Infectious HCV culture systems were used to evaluate the influence of SB-NP on the virus life cycle and examine their antioxidant activity against HCV induced oxidative stress. The safety profiles of SB-NP, in vivo pharmacokinetic studies and antiviral activity against infection of primary human hepatocytes were also assessed.SB-NP consisted of nanoscale spherical particles (<200 nm) encapsulating amorphous silibinin at >97% efficiency and increasing the compound's solubility by >75%. Treatment with SB-NP efficiently restricted HCV cell-to-cell transmission, suggesting that they retained silibinin's robust anti-HCV activity. In addition, SB-NP exerted an antioxidant effect via their free radical scavenging function [27].

Nagesh *et.al,* (2016) develop and determine the anti-cancer efficacy of a novel docetaxel loaded, prostate specific membrane antigen (PSMA) targeted superparamagnetic iron oxide nanoparticle (SPION) formulation for prostate cancer (PC) therapy. Docetaxel (Dtxl) is currently the most common therapeutic option for prostate cancer (PC). The adverse side effects and problems associated with chemo-resistance limit its therapeutic outcome in clinical settings. The results showed the SPION-Dtxl formulation exhibits an optimal particle size and zeta potential, which can efficiently be internalized in PC cells. SPION-Dtxl exhibited potent anti-cancer efficacy via induction of the expression of apoptosis associated proteins, downregulation of anti-apoptotic proteins, and inhibition of chemo-resistance associated protein in PC cell lines[32].

Mishra *et.al,* (2016) reviewed Targeted drug delivery, also known as smart drug delivery, is a method of treatment that involves the increase in medicament in one or few body parts in comparison to others. Two strategies are widely used for drug targeting to the desired organ/tissue: passive targeting and active targeting. Drug delivery vehicles transport the drug either within or in the vicinity of target. An ideal drug delivery vehicle is supposed to cross even stubborn sites such as a blood brain barrier. Recently, nano medicine has emerged as the medical application of nanotechnology. Since nanoparticles are very small in size, nano drug delivery can allow for the delivery of drugs with poor solubility in water and also aid in avoiding the first pass metabolism of liver. Nanotechnology derived drug delivery can cause the drug to remain in blood circulation for a long time, thereby leading to lesser fluctuations in plasma levels and therefore, minimal side effects. These include polymer-drug conjugates and nano particulate systems such as liposomes, quantum dots, dendrimers, etc. There are several other approaches as well. These also include the strategies wherein the therapeutic agents are coupled with "targeting ligands" that possess the ability to recognize antigens associated with tumors[38].

Mir *et.al,* (2016) studied the Comparative Modeling and Molecular Docking Study of P53 and AKT1 Genes of Lung Cancer Pathways. It has been assumed that current study will play a significant contribution to design potential drug inhibitors by utilizing most interactive residue information with Nutlin-3 and Staurosporine ligands to restrain the interaction between p53 pathways and epidermal growth pathways. The endeavor behind this work is to select most susceptible genes p53 and AKT1 which plays a vital role in lung cancer pathogencity. In a queue to deliberate the crucial role of these genes in-silico experimental strategy was adopted. 3-D structure of p53 generated by YASARA showed 50.9% sequence identity with 2PCX-A and Z-score of -0.276 while AKT1 showed 66.3% sequence identity with 3QKL-A and Z-score of 0.036. Mutational analysis revealed that R273L and C275Y mutations of p53 destabilize the DNA binding domain, while E17K mutation of AKT1directly affect the binding of the ligand as this residues lines the pocket. Molecular docking was performed using ligands Staurosporine and Nutlin-3 retrieved form ZINC database. Blind docking experiment revealed that p53 involve non polar (Leu206, Leu188, Pro190), acidic (Glu204, Tyr 205) and basic (Arg202) as most interacting residues. AKT1 interactions with ligand Staurosporine revealed nonpolar (Val164, Phe438, Phe442, Phe 236, Phe 237, Phe 161), polar (Gly159, Gly157, Gly234, Gly 278), basic (Lys163, Lys158, Lys 276, Lys 179), acidic (Asp439, Glu278) as most interacting residues[45].

Yazdani *et.al,* (2016) synthesized magnetic nanoparticle by co-precipitation method. Magnetite nanoparticles due to the special specifications have been widely used in medical as well as industrial applications. In such applications, it is important to control morphology and size of the nanoparticles. Magnetite nanoparticles were synthesized using different precursor salts. For investigating the effect of various precursors on mean size and morphology of synthesized nanoparticles, six groups of magnetite precursors were arranged. The magnetite product of each group was characterized by using XRD, SEM, TEM, VSM and the analytical methods. Kind of precursors influence on the mean size of the synthesized nanoparticles. Nanoparticles mean size decreases as the anion size of the precursor increases. The reason for this behavior was explained by the double layer theory. However, kind of precursors did not have a sensible effect on the morphology of the synthesized nanoparticle[52].

Saiyyad *et.al,* (2017) prepared silymarin loaded PLGA polymeric nanoparticles for liver targeting by solvent evaporation method. PLGA were employed as a bio-degradable polymer for targeting and controlled release of drug. The particle size was mainly controlled by the agitation speed during the manufacturing process and polymer concentration. As PLGA nanoparticles have the stability problem hence PVA used as Surfactant as well as Stabilizing agent for the production of stable nanoparticles. Further it is characterization such as particle size, zeta potential, and DSC and SEM analysis. Particle Size in between 422.4-294.3 nm. Entrapment Efficiency in between 74.30-99.8% and % drug release in between 73.53-98.67% which follows the sustained release behaviour. This study concluded that Nanoparticle containing PLGA exhibiting excellent sustained release characteristics and Entrapment efficiency and also Good particle Size [31].

Hamzian *et.al,* (2017) developed a novel multifunctional nanoparticle, which encapsulates SPION and Gemcitabine in PLGA ± PEG to form multifunctional drug delivery system. In this super paramagnetic iron oxide nanoparticles (SPIONs) were simultaneously synthesized and encapsulated with Gemcitabine (Gem) in PLGA ± PEG copolymers via W/O/W double emulsification method. This optimization was designed based on applications such as radio sensitization, hyperthermia and ultrasound and MR imaging by contrast agents. The hydrodynamic diameters of all nanoparticles were under 200 nm. Encapsulation efficiency was adjusted between 13.2% to 16.1% for Gemcitabine and 48.2% to 50.1% for SPION [7].

wu *et.al,* (2017) reviewed that magnetic nanoparticles(MNPs) have demonstrated marked progress in the field of oncology research on MNPs in cancer diagnosis, drug delivery and treatment has been summarized. General nanoparticles are widely used in tumour targeting,

and the intrinsic magnetic property of MNPs makes them the most promising nanomaterial to be used as contrast agents for magnetic resonance imaging (MRI) and induced magnetic hyperthermia. The properties of MNPs are fully exploited when they are used as drug delivery agents, wherein drugs may be targeted to the desired specific location in vivo by application of an external magnetic field. Early diagnosis of cancer may be achieved by MRI, therefore, individualized treatment may be combined with MRI, so as to achieve the precise definition and appropriate treatment[35].

Amirsaadat *et.al,* (2017) had fabricated and characterized silibinin-loaded magnetic nanoparticles and evaluated cytotoxicity and hTERT gene expression in A549 lung cancer cell line. Nanoparticle-based targeted drug delivery has the potential for rendering silibinin specifically at the favorite site using an external magnetic field. Also, it can circumvent the pitfalls of poor solubility. For this purpose silibinin-loaded PLGA-PEG-Fe3O4 had dose- and time-dependent cytotoxicity than pure silibinin. Additionally, hTERT expression is more efficiently reduced with increasing concentrations of nanosilibinin than pure silibinin. The present study indicates that PLGA-PEG-Fe3O4 nanoparticles, as an effective targeted carrier, can make a promising horizon in targeted lung cancer therapy[36].

Zheng *et.al.*, (2018) discussed about various preparation methods of Super paramagnetic iron oxide nanoparticle (SPIONs) include co precipitation method, high thermal decomposition, hydrothermal reaction and microwave irradiation. Further surface modification of SPIONs for further imaging and therapy done by mesoporous silica, PEG, PVA, dextran and albumin. The biomedical applications of MNPs, which includes applications in targeted drug delivery, diagnostics, gene therapy, hyperthermia and advantages in the field of medicine [29].

Binandeh *et.al.*, (2020) synthesized iron oxide nanoparticle and identified by SEM, FT-IR, and EDX analyzers and finally reacted with the BSA protein (for the absorption of protein on MNPs) under experimental conditions at a standard temperature of 25° C. The nanoparticles synthesized in this work were deposited by the co-precipitation method, which structure was identified by analyzers such as SEM, FT-IR, and EDX. The adsorption and fixation of biomolecule (BSA (bovine serum albumin) protein on the surface of magnetic nanoparticles. The adsorption results by electrophoresis and spectrophotometric analyzers showed an absorption rate above 55% of the protein is fixed on the MNPs nanoparticles. This absorption is due to the high level of functionality of magnetic nanoparticles for adsorption of protein. The results of the EDX analysis also show the possible electrostatic bonding between the

nanoparticles and the protein, this is derived from –OH with –NH2 groups of the nano biocompound (MNPs /protein). After bonding, the two are easily separated[40].

Palestino *et.al,* (2020) reviewed the current COVID-19 pandemic caused by the SARS-CoV-2 virus demands the development of strategies not only to detect or inactivate the virus, but to treat it (therapeutically and prophylactically). COVID-19 is not only a critical threat for the population with risk factors, but also generates a dramatic economic impact in terms of morbidity and the overall interruption of economic activities. Advanced materials are the basis of several technologies that could diminish the impact of COVID-19: biosensors might allow early virus detection, nanosized vaccines are powerful agents that could prevent viral infections, and nano systems with antiviral activity could bind the virus for inactivation or destruction upon application of an external stimulus. Perspectives on how biosensors, vaccines, and antiviral nano systems can be implemented to fight COVID-19 are envisioned; identifying the approaches that can be implemented in the short term and those that deserve long term research to cope with respiratory viruses-related pandemics in the future[42].

Weiss *et.al.,* (2020) The COVID-19 outbreak has fuelled a global demand for effective diagnosis and treatment as well as mitigation of the spread of infection, all through large-scale approaches such as specific alternative antiviral methods and classical disinfection protocols. By considering about the life cycle of the virus, we envision key steps where nanotechnology could counter the disease. Nanotechnology tools to inactivate SARS-CoV-2 in patients could also be explored. In this case, nanomaterials could be used to deliver drugs to the pulmonary system to inhibit interaction between angiotensin-converting enzyme 2 (ACE2) receptors and viral S protein. Moreover, the concept of "nano immunity by design" can help us to design materials for immune modulation, either stimulating or suppressing the immune response, which would find applications in the context of vaccine development for SARS-CoV-2 or in counteracting the cytokine storm, respectively. In addition to disease prevention and therapeutic potential, nanotechnology has important roles in diagnostics, with potential to support the development of simple, fast, and cost-effective nanotechnology-based assays to monitor the presence of SARS-CoV-2 and related biomarkers. In summary, nanotechnology is critical in counteracting COVID-19 and will be vital when preparing for future pandemics[4].

Chakravarty *et.al.,* (2020) reviewed Nanotechnology bases for antiviral therapeutics. Nanotechnology has emerged as one of the most promising technologies on account of its ability to deal with viral diseases in an effective manner, addressing the limitations of traditional antiviral medicines. It has not only helped us to overcome problems related to

solubility and toxicity of drugs, but also imparted unique properties to drugs, which in turn has increased their potency and selectivity toward viral cells against the host cells. The host immune system is highly compromised in case of viral infections and relapses are very common. The capacity of the virus to destroy the host cell by liberating its own DNA or RNA and replicating inside the host cell poses challenges in the development of antiviral therapeutics. The initial part of this paper focuses on some important proteins of influenza, Ebola, HIV, herpes, Zika, dengue, and corona virus and those of the host cells important for their entry and replication into the host cells. This is followed by different types of nanomaterials which have served as delivery vehicles for the antiviral drugs. It includes various lipid-based, polymer-based, lipid–polymer hybrid–based, carbon-based, inorganic metal–based, surface-modified, and stimuli-sensitive nanomaterials and their application in antiviral therapeutics. The authors also highlight newer promising treatment approaches like nanotraps, nanorobots, nanobubbles, nanofibers, nanodiamonds, nanovaccines, and mathematical modeling for the future. The paper has been updated with the recent developments in nanotechnology-based approaches in view of the ongoing pandemic of COVID-19 [43].

Subashini *et.al.*, (2021) reviewed the prospective treatment options integrating the ever-expanding field of nanotechnology against COVID-19. The current scenario in the developments of nanotechnology based approaches because of the ongoing pandemic of COVID-19, the effectiveness of nanomaterials as vaccines, nano sensors as diagnostic or antiviral tools against coronaviruses, and post COVID-19 era has been discussed in this review. Coronavirus disease (COVID-19), an infectious disease caused by a novel coronavirus (2019-nCoV) or the severe acute respiratory syndrome coronavirus 2 (SARS-CoV-2). The infection began in bats and was communicated to people through yet obscure go-between creatures in Wuhan, Hubei territory, China, in December 2019. Its outbreak threatened the lives of many people throughout the world. There is no distinct treatment available yet, and is an urgent need to treat, prevent and eradicate this virus. Recently, numerous new technologies have been explored for the diagnosis, prevention, and treatment of viral infections. Among these, nanotechnology has emerged as a promising antiviral treatment, and currently, the development of COVID-19 drug delivery involving nanotechnology is under investigation[41].

Hanafy *et.al.*, (2022) has worked on Silymarin/curcumin loaded albumin nanoparticles coated by chitosan as muco-inhalable delivery system observing Anti-inflammatory and Anti-COVID-19 characterizations in oleic acid triggered lung injury and in vitro COVID-19 experiment. Respiratory infected by COVID-19 represents a major global health problem at

moment even after recovery from virus corona. Since, the lung lesions for infected patients are still sufferings from acute respiratory distress syndrome including alveolar septal edema, pneumonia, hyperplasia, and hyaline membranes Therefore, there is an urgent need to identify additional candidates having ability to overcome inflammatory process and can enhance efficacy in the treatment of COVID-19. The polypenolic extracts were integrated into moeties of bovine serum albumin (BSA) and then were coated by chitosan as a mucoadhesion polymer.The results of interleukin-6, and c-reactive protein showed significant reduction in group treated by Encap. SIL + CUR (64 ± 0.8 Pg/µL & 6 ± 0.5 µg/µL) compared to group treated by Cham. + CUR (102 ± 0.8 Pg/µL & 7 ± 0.5 µg/µL) respectively and free capsules (with no any drug inside) (148 ± 0.6 Pg/µL & 10 ± 0.6 µg/µL) respectively. Histopathology profile was improved completely. Additionally, encapsulating silymarin showed anti-viral activity *in vitro* COVID-19 experiment. It can be summarized that muco-inhalable delivery system (MIDS) loaded by silymarin can be used to overcome inflammation induced by oleic acid and to overcome COVID-19 [48].

Nemany A.N. Hanafy and Maged A. El-Kemary (2022) worked on encapsulating silymarin showed anti-viral activity in vitro COVID-19 experiment. It can be summarized that muco-inhalable delivery system (MIDS) loaded by silymarin can be used to overcome inflammation induced by oleic acid and to overcome COVID-19. Respiratory infected by COVID-19 represents a major global health problem at moment even after recovery from virus corona. Since, the lung lesions for infected patients are still sufferings from acute respiratory distress syndrome including alveolar septal edema, pneumonia, hyperplasia, and hyaline membranes. Therefore, there is an urgent need to identify additional candidates having ability to overcome inflammatory process and can enhance efficacy in the treatment of COVID-19. The polypenolic extracts were integrated into moeties of bovine serum albumin (BSA) and then were coated by chitosan as a mucoadhesion polymer. The results of interleukin-6, and c-reactive protein showed significant reduction in group treated by Encap. SIL + CUR (64 ± 0.8 Pg/µL & 6 ± 0.5 µg/µL) compared to group treated by Cham. + CUR (102 ± 0.8 Pg/µL & 7 ± 0.5 µg/µL) respectively and free capsules (with no any drug inside) (148 ± 0.6 Pg/µL & 10 ± 0.6 µg/µL) respectively. Histopathology profile was improved completely[50].

Aim and Objective

AIM AND OBJECTIVE

- The aim of this project is to contribute to the search for potential drug targeting formulation for covid-19, the pandemic of the current situation that has taken 23.68 lakhs of human lives and infected 10.80 million people globally.
- To determine the binding ability of silymarin with the receptor by molecular docking.
- To target the affected site of lung for better bioavailability and to reduce the further toxicity.
- To prepare super paramagnetic iron oxide nanoparticle (SPION) as a targeting system to act as a drug carrier for SARS-COV-2.
- To characterize the silymarin loaded super para magnetic iron oxide nanoparticle (SPION)

Plan of Work

PLAN OF WORK

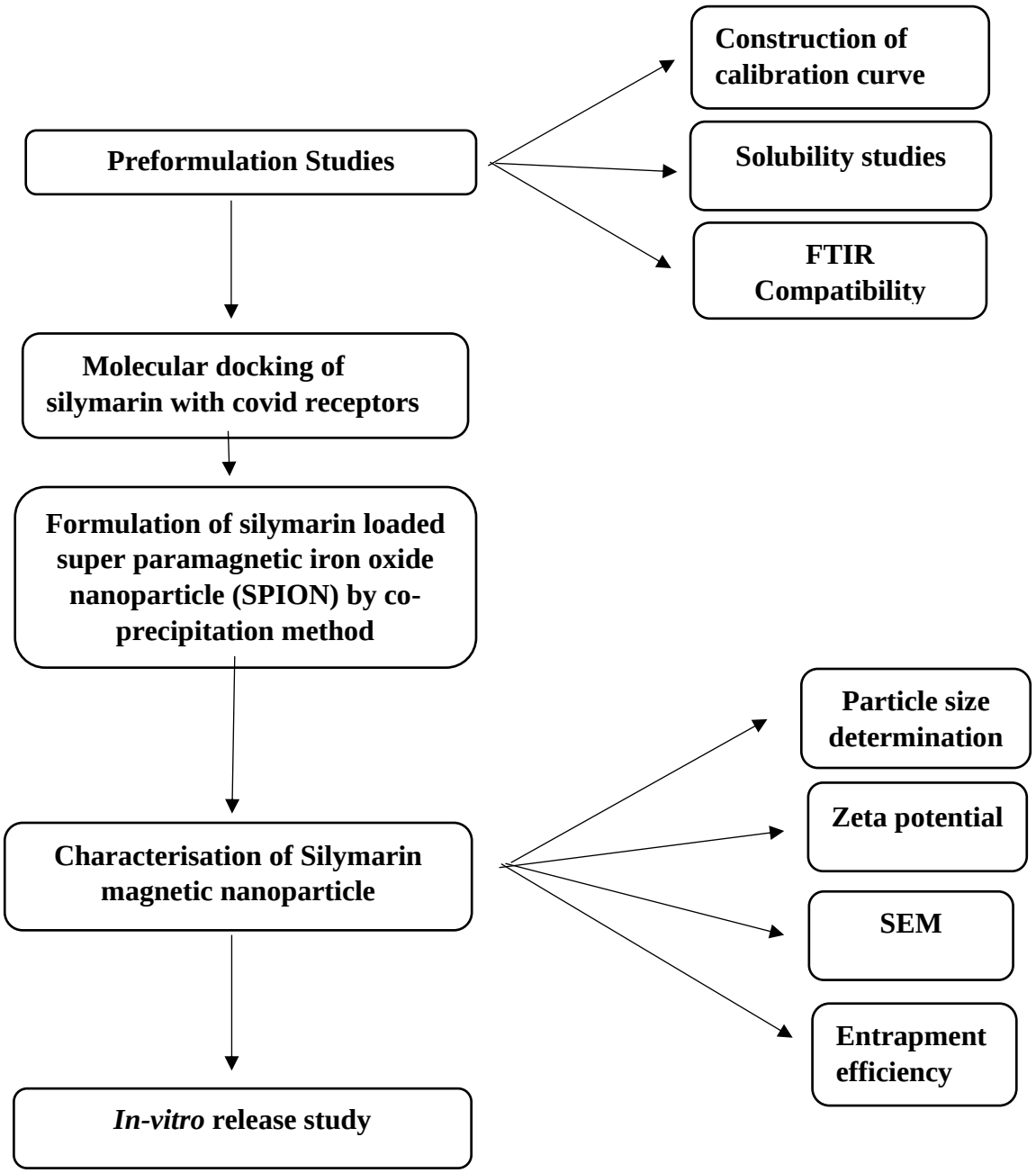
Preformulation Studies
Construction of calibration curve
Solubility studies
FTIR Compatibility
Molecular docking of silymarin with covid receptors
Formulation of silymarin loaded super paramagnetic iron oxide nanoparticle (SPION) by co-precipitation method
Characterisation of Silymarin magnetic nanoparticle
Particle size determination
Zeta potential
SEM
Entrapment efficiency
In-vitro release study

Materials & Equipments

MATERIALS AND EQUIPMENTS

MATERIALS USED

Sl. No	Materials	Source
1.	Silymarin	Gift sample
2.	Ethyl Cellulose	Himedia, Mumbai
3.	Eudragit	Yarrow Pharma
4.	Poly Ethylene Glycol (1000)	Lancaster synthesis
5.	Ammonium hydroxide	Lobachemie Pvt, Ltd, Mumbai
6.	Ferrous chloride	Himedia, laboratories Pvt, Ltd Nasik
7.	Ferric chloride	Himedia, laboratories Pvt, Ltd Nasik
8.	Oleic acid	Lobachemie Pvt, Ltd, Mumbai
9.	Ethanol	Zhuhai Chemico Industries
10.	Poly vinyl alcohol	Himedia, Mumbai
11.	Disodium hydrogen phosphate	SD Fine Chemical Limited
12.	Potassium dihydrogen phosphate	Qualigens Fine Chemicals, Mumbai
13.	Sodium hydroxide	Lobachemie Pvt, Ltd, Mumbai

EQUIPMENTS USED

Sl. No	Equipment	Model/ Company
1.	Magnetic Stirrer	REMI-2MLH
3.	UV Spectrophotometer	JASCO V-530
4.	FT-IR Spectrometer	FTIR JASCO -4100
5.	pH Meter	pH TESTER 1,2(EUTECH)
6.	Zeta Sizer	MALVERN
7.	SEM	Joel model JSM 6400, Tokyo
8.	Dialysis membrane 50mm	Himedia, Mumbai
9.	Molecular docking	Discovery studio 2021, Auto dock 1.5.6, Cygwin 64 terminal
10.	DD Solver	Microsoft

Drug Profile

DRUG PROFILE

SILYMARIN

Description:

Silymarin is an active component obtained from the plant Silybum marianum, commonly known as milk thistle from the family Asteraceae. About 70-80% of the plant consists of silymarin flavinolignan i. e silidianin, silychristin, silybin A and B and iso silybin A and B.

IUPAC name: 2-(2,3-Dihydro-2-(4-hydroxy-3-methoxyphenyl)-3-(hydroxyl methyl)-1,4-benzodioxin-6-yl)-2,3-dihydro-3,5,7-trihydroxy-4H-1-benzopyean-4-one.

Empirical formula: C25H22O10

Molecular weight: 482.436

Melting point: 164-174ºC

Boiling point: 793ºC at 760mm Hg

Density: 1.527g/cm3

Colour: light yellow powder

Solubility: solubility of silymarin in various solvents is given in Table 1.

Table1: Solubility of Silymarin in Various Solvents

Transcutol	350.1 mg/ Ml
Ethanol	225.2 mg/ mL
Polysorbate 20	131.3 mg/ mL
Glyceryl monooleate	33.2 mg/ mL
Water	0.04 mg/ mL

Categories:

Hepatoprotective, antioxidative, anti -inflammatory, neuroprotective, neurotropic, antilipid peroxidative, cardioprotective and membrane stabilizing agent.

Mechanism of Action:

• Silymarin due to its property of free radical scavenging can act against lipid per oxidation and also helps to increase cellular content of Glutathione.

• During xenobiotic damage it regulates membrane permeability resulting in better membrane stability.

• Silymarin has asteroid like effect which helps in regulating nuclear expression. The conversation of stellate hepatocytes to myofibroblast which is known factor for cirrhosis is inhibited by silymarin.

Adverse Reactions:

Nausea, diarrhoea, indigestion, flatulence, bloating, fullness or pain, anorexia, occasional laxative effects. It is well-known to cause allergic response in people who are sensitive to Asteraceae/ Compositae family.

Dosage and administration:

Oral; hepatic diseases: adult 70-140mg bid/tid

Absorption:

Absorption of silymarin is comparatively low after oral administration i.e about 20-30%. Peak plasma concentrations are achieved within 4-6 hrs.

Metabolism:

In the liver silymarin gets conjugated with sulphates and glucuronic acid and then conjugates passes through plasma and bile.

Elimination:

Silymarin is mainly excreted in bile and to lesser extent in urine. The elimination half -life is silymarin is 1-3 hrs.

Indications:

Silymarin is used to treat hepatitis, as an adjunctive therapy in the treatment of cirrhosis, jaundice and also in alcohol related liver diseases. It has also found to possess anticancer activity.

Contraindications:

Silymarin is contraindicated in cases of hypersensitivity, hepatic encephalopathy, and primary biliary cirrhosis and in cases of hypersensitivity to components of silymarin.

Storage and Handling:

Store in a well closed container in a cool, dry and dark place.

Brand names:

Silymarin marketed product given in Table 2.

Table 2: Marketed Products of Silymarin

Brand names	Manufacturer's
C. Hepasil	*Signova*
C. Levalon	*Micro B&B*
C.Levalon	*Serum Intl.*
C.Prohepforte	*LUPIN*
C.Silimar	*Zydus(G.Rem)*
C.Sison	*Dr. Alson Labs*

Polymer Profile

EXCIPIENT PROFILE

ETHYL CELLULOSE

Non proprietary names

BP: Ethylcellulose

PhEur: Ethylcellulosum

USPNF: Ethylcellulose

Synonyms

Aquacoat; E462; Ethocel; Surlease

Chemical names and CAS registry number

Cellulose ethyl ether [9004-57-3]

Empirical formula

Ethyl cellulose is an ethyl ether of cellulose, a long chain polymer consisting of anhyroglucose units joined by acetate linkage. Each anhydroglucose units has three replacable hydroxyl groups which are substituted to the extent of 2.25-2.60 ethoxul groups(OC_2H_5) per unit, equivalent to an ethoxyl content of 44-51%

Structural formula

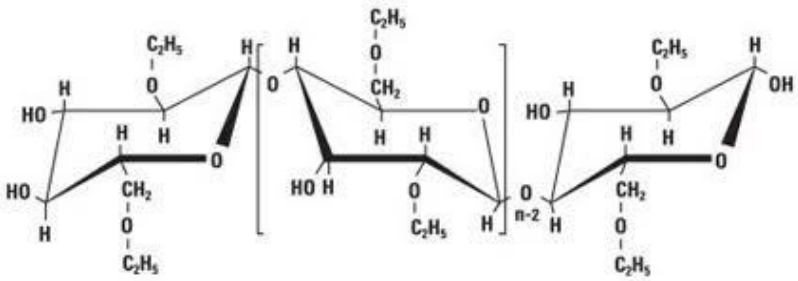

Functional category

Coating agent; tablet binder; viscosity increasing agent

Applications in pharmaceutical formulation or technology

Ethyl cellulose is widely used in oral and topical pharmaceutical formulations. The main use of ethyl cellulose in oral formulations is as a hydrophobic coating agent for tablet and granules.Ethyl cellulose coatings are used to modify the release of a drug, to mask an unpleasant taste, or to improve the stability of the formulations. Higher viscosity ethyl cellulose grades tend to produce stronger, tougher films. Ethyl cellulose is also widely used in drug microencapsulation, high viscosity grades usually being used.

Description

Ethyl cellulose is a tasteless, free flowing, white or light tan coloured powder.

Typical properties

Density:

0.4g/cm^3

Glass transition temperature:

130-133^{0}C

Melting point:

165-173^{0}C

Hygroscopicity:

Ethyl cellulose absorbs very little water at high relative humidity or during immersion.

Solubility:

Practically insoluble in glycerine, propylene glycol and water. Ethyl cellulose that contain not less than 46.5% of ethoxyl group is freely soluble in chloroform, ethanol, ethyl acetate, methanol and toluene.

Specific gravity: 1.12-1.15

Viscosity:

Various grades of ethyl cellulose are commercially available having viscosities ranging from 3-385MPas.

Stability and storage conditions

Ethyl cellulose is a stable, slightly hygroscopic material. It is chemically resistant to alkalis, both dilute and concentrated, and to salt solutions, though it is more sensitive to acidic materials than cellulose esters. Ethyl cellulose is subject to oxidative degradation in the presence of sunlight or UV light at elevated temperatures.

The bulk material must be stored in a dry place, in a well closed container at a temperature between 7-32^{0}C.

Incompatibilities

Incompatible with paraffin wax and microcrystalline wax.

Method of manufacture

Ethyl cellulose is prepared from wood pulp by treatment with alkali followed by ethylation of alkali cellulose with chloroethane.

Safety

Ethyl cellulose is widely used in oral and topical pharmaceutical formulations. It is also used in food products. It is generally regarded as a nontoxic, non-allergenic and non-irritant material.

Handling precautions

Observe normal precautions appropriate to the circumstances and quantity of materials handled. Dust may be irritant to the eyes and eye protectant should therefore be worn. Ethyl cellulose is combustible.

EUDRAGIT

Chemical name: methacrylic acid

Chemical formula: $C_4H_6O_2$

Chemical Structure:

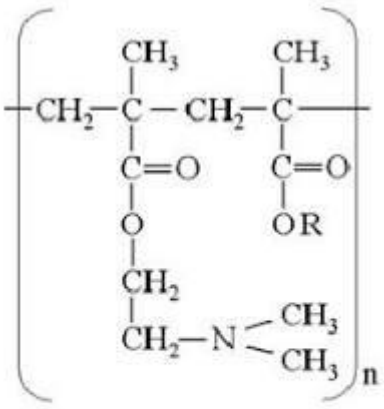

R = CH_3, C_4H_9

Synonyms:

- 2-(methoxycarbonyl)-1-propene
- 2-methyl-2-propenoic acid methyl ester

Appearance:

Colourless

Odour:

Unpleasant, acrid and repulsive.

Solubility:

Soluble in warm water

Miscible with most organic solvents

Density:

1.02g/cm^3

Molar mass:

86.06g/mol

Boiling point:

161^0C

Melting point:

15^0C

Applications

- Ophthalmic drug delivery
- Buccal and sublingual drug delivery
- Gastrointestinal drug delivery
- Intestinal drug delivery
- Colon drug delivery
- Transdermal drug delivery
- Vaginal drug delivery
- Gene drug delivery
- Vaccine drug delivery

Eudragit polymer were selected for these studies because they dissolved at pH > 5.5 and are not soluble in acidic gastric fluid and which can prevent the premature release of the incorporated drug molecule during the preparation before dosing.

Eudragit are sufficiently being used in pre-clinical models to enable *in vivo* safety pharmacology studies where small changes in organ function and physiology are assessed during lead optimization.

Method of Manufacture

In one route, acetone cyanohydrin is converted to meth acrylamide sulphate using sulphuric acid which is then hydrolysed to methacrylic acid. In the second route, isobutylene or tert-butanol are oxidised to methacrolein, then methacrylic acid.

POLYETHYLENE GLYCOL

IUPAC Names:

Poly (oxyethylene) {structure-based}, Poly (ethylene oxide){source-based}

Other Names:

Carbowax, Golytely, Glycolax, Fortrans, Trilyte, Colyte, Halflytely, Macrogol, Miralax, Moviprep.

Chemical formula: $C_{2n}H_{4n+2}O_{n+1}$

Molar mass: $18.02+44.05_n$ g/mol

Flash point: 182 to 287°c; 360 to 549°F; 455 to 560K

Molecular weight:

300 g/mol to 10,000,000 g/mol.

Chemical Structure:

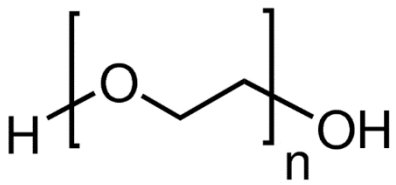

Description

PEG and PEO with different molecular weight find use in different application, and have physical properties (e.g. viscosity) due to chain length effect; their chemical properties are nearly identical. Different forms of PEG are also available, depending on the initiator used for the polymerization process –the most common initiator is a mono functional methyl ether PEG,or methoxypoly (ethylene glycol), abbrivated mPEG . Lower-molecular-weight PEGs are available as purer oligomers, referred to as monodisperse, uniform, or discrete. Very high purity PEG has recently been shown to be crystalline, allowing determination of a crystal structure by x-ray diffraction. Since purification and separation of pure oligomers is difficult, the price for this type of quality is often 10-1000 fold that of polydisperse PEG.

Solubility:

PEG is soluble in water, methanol, ethanol, acetonitrile, benzene and dichloromethane, and insoluble in diethyl ether and hexane. It is coupled to hydrophobic molecule to produce non ionic surfactants.

Incompatibility:

PEG contain potential toxic impurities, such as ethylene oxide and 1, 4 dioxane. Ethylene glycol and its ethers are nephrotoxic if applied to damaged skin.

Application in pharmaceutical formulation or technology

PEGs and methoxy polyethylene glycols are manufactured by Dow chemical under the trade name Carbowax for industrial use, and Carbowax Sentry for food and pharmaceutical use. They vary in consistency from liquid to solid, depending on the molecular weight, as indicated by a number of following the name. They are used commercially in numerous applications, including as surfactants, in foods, in cosmetics, in pharmaceutics in biomedicine, as dispersing agents, as solvents, in ointment, in suppository bases, as tablet excipients, and as laxatives. Some specific groups are louromacrogols, nonoxynols, octoxynols and poloxamers. Macrogols, used as a laxative, is a form of polyethylene glycol.The name may be followed by a number which represents the average molecular weight (Example ;macrogol 4000, macrogol 3350 or macrogol 6000).

Method of Manufacture

PEGs are prepared by polymerization of ethylene oxide and are commercially available over a wide range of molecular weight

Experimental Methods

EXPERIMENTAL METHODS

PREFORMULATION STUDIES:

Physical characteristics:

By visual examination the drug was tested for its physical characters like colour, odour and texture.

Solubility test:

Silymarin powder (about 1mg) was weighed in a test tube and solubility in ethanol, water, dichloromethane and chloroform was tested.

Max determination

Preparation of stock solution

The standard stock solution of silymarin was prepared by transferring accurately weighed quantity (10 mg) of silymarin raw material in 100 ml of volumetric flask. The drug was dissolved in few ml of ethanol and the volume was made up to 100 ml with ethanol to get a stock solution of 100 µg/mL.

Selection of Wavelength

The standard stock solution was scanned in the range of 200 to 400 nm in UV spectrophotometer using phosphate buffer pH 6.8 as blank. The absorption maximum was found at 288 nm.

Construction of calibration curve of silymarin:

From the standard stock solution of silymarin 1,2,3,4 and 5 ml were withdrawn to 10 ml volumetric flask and then made-up volume with phosphate buffer pH 6.8 to get a concentration range of 5-40 µg/ml. The absorbance of these solutions was measured at 288nm using JASCO V-530 UV 1600 UV- visible spectrophotometer. Phosphate buffer pH 6.8 was used as blank. The calibration curve was plotted between concentration and absorbance [53].

Preparation of Buffer Solutions

Phosphate buffer pH 6.8: An accurately weighed quantity of 28.80gm of disodium hydrogen phosphate and 11.45gm of potassium dihydrogen phosphate was dissolved in sufficient water to produce 1000ml [54].

PREPARATION OF SUPERPARAMAGNETIC IRON OXIDE NANOPARTICLES (SPIONS)

SPIONs were synthesized using a co-precipitation method. Briefly, 450 ml of deionized water was stirred mechanically for 15 min under a nitrogen gas at room temperature to remove oxygen from solution. Then 0.19 mg Ferric chloride and 0.486 mg Ferrous chloride were added to the vigorously stirred water and 250 mg of oleic acid was quickly added to the previous reaction mixture and the product container was placed in a water bath (75-80˚C). After 15 min, 1.35 ml of Ammonium hydroxide was added during one minute and argon gas flow was discontinued. After about 30 min, SPIONs were deposited. The product was washed three times with deionized water and the black precipitate was separated using a permanent magnet and lyophilized [7].

ENCAPSULATION OF SILYMARIN IN SPIONS

Double emulsion method (W1/O/W2) was used for preparation of SPION encapsulated with silymarin using Ethyl cellulose, Eudragit, Poly ethylene Glycol (PEG). Briefly, 1 ml of SPION suspension in chloroform was mixed with 1 ml of the organic solution of the polymer in dichloromethane. Then, 0.2 ml solution of silymarin in deionized water was added to the organic phase, and the mixture was emulsified by sonication for 1 min (0.6 Hz frequency, 90 amplitude) (W/O). The primary water-in-oil (W/O) emulsion was added drop wise to 8 ml of ice-cold aqueous Poly vinyl alcohol solution (5%, W/V) and emulsified for 10 min using a probe sonicator (W1/O/W2). To evaporate the organic solvent, the resulted solution was diluted in 10 ml aqueous Poly vinyl alcohol solution (0.1%, w/v) under stirring at room temperature overnight. Then the nanoparticles were collected by centrifugation at 14000 rpm for 15 min and washed three times with deionized water. Finally, the products were freeze-dried and the dry samples were filled with N2 gas and stored in a freezer for further use[7].

MOLECULAR DOCKING STUDY

Molecular docking analysis performed to evaluate the most preferred geometry of the protein ligand complex. Docking phase is meaningless without its two components such as target protein and ligand. Homosapien covid receptors were used for performing docking study as target proteins. Docking results identify native or native-like configurations of the protein-ligand complex. Various Homosapen receptor were selected and docked. The best binded

receptors were further compared with the standard ligand. Remdesivir is the selected standard as it is the most potent currently used Anti-viral drug.

Accession of target protein

The three-dimensional structure of the Homosapen receptor of covid (PDB:6VYB, 7LMF, 6LU7, 4RNA, 7JMP, 6ML7, 6ZGE, 7JMO, 6ZGG, 5N11, 7LQW, 6VXX, 6CRV) was retrieved from the RCSB protein Data Bank[55].

Ligand selection

The chemical structure of Silymarin and Remdesivir was obtained from PubChem compound database. The collected Structure Data File (SDF) files of these compounds from the PubChem database were converted into PDB format using online smile translator in google[55].

Target and ligand optimization

For docking analysis, PDB coordinates of the target protein and Silymarin, Remdesivir molecule were optimized by Drug Discovery Studio version 2021 software. These coordinates had minimum energy and stable conformation[56].

Analysis of target active binding sites

The active sites are the coordinates of the ligand in the original target protein grids, and these active binding sites of target protein were analysed using the Drug Discovery Studio version 2021.

Protein ligand docking

Molecular docking analysis performed to evaluate the most preferred geometry of the protein ligand complex. Docking phase is meaningless without its two components such as target protein and ligand. Homosapien covid receptors were used for performing docking study as target proteins. Docking results identify native or native-like configurations of the protein-ligand complex. The selected proteins complex used after removal of already bonded ligand and water molecules. Docking was performed by AutoDock 1.5.6 software. The complete docking steps could be stated as follows: first of all, the water molecules were eliminated from the protein. After the removal of water molecules, the PDB file of those covid receptor protein which were provided as an input to the software. Kollman charges were computed for the

macromolecule by AutoDock. Then the macromolecule was checked for the missing atoms and repaired. After repairing missing atoms, the hydrogens were added by keeping all the parameters at default settings. The macromolecule after all these modifications was saved as PDB in the same directory. Then the ligand preparation was carried out. Like macromolecule, Kollman and Gasteiger charges were computed for the ligand. Some of the torsions of the ligands were defined. The root was detected; the rotatable bonds were converted into non-rotatable bonds and vice versa. And the number of active torsions was to the most atoms rather than fewest. A Protein Data Bank, Partial Charge (Q) and Atom Type (T) (PDBQT) file was then created for the modified ligand with extension PDBQT. After the preparation of a macromolecule and ligand, the rigid residue was prepared using the grid module provided in the AutoDock 1.5.6 Grid module employed PDB file. This program was run using a searching grid extended over ligand molecules with box spacing 90×70×60; spacing was 0.808, x, y, z coordinates 8.485, -5.766, 15.737 respectively for all those receptor proteins while other parameters were default. The flexible macromolecule was saved with the PDBQT extension. For molecular docking AutoDock 1.5.6 software was used. It employed a configuration file referring to PDBQT files of macromolecules and compounds prepared using AutoDock 1.5.6 and grid properties. As an output AutoDock 1.5.6 generated log files and PDBQT files of energy models for the selected data set. The output file contained different energy models. Among these models, the lowest energy model against each ligand was selected and appended at the end of the original protein file. As a result of this step, docked files for the selected set were generated. For the interpretation of docking results; target protein and protein docked with the data set of compounds, the interactions between the active pocket of protein and compounds were found. The best docking poses were predicted to be the most stable conformation of each compound for binding to the protein active site. Consequently, the output of the docking process was analyzed utilizing Autodock 1.5.6[56].

CHARACTERISTICS OF SPIONS

FTIR Spectroscopy of Nanoparticle

A few mg of sample (silymarin nanoparticle) was weighed and mixed with 100 mg of potassium bromide (dried at 40-50ºC). The mixture was taken and compressed under 10- ton pressure in hydraulic press to form a pellet. The pellet was scanned from 4000-400 cm^{-1} in IR spectrophotometer.

Determination of Percentage Yield

Silymarin loaded nanoparticle were weighed after drying. Percentage yield was calculated by

$$\%\ yield = \frac{Practical\ weight\ of\ nanoparticle\ obtained}{Theoretical\ weight(\ drug + polymers)} \times 100$$

Morphology by scanning electron microscopy (SEM)

The morphology of SPIONs was analyzed by scanning electron microscope (JEOL MODEL JSM 6400). The SPIONs were mounted directly on the SEM stub, using double – sided, sticking tape and coated with platinum and scanned in a high vacuum chamber with a focused electron beam. Secondary electrons, emitted from the samples were detected and the image formed[7].

Surface characteristics by zeta sizer

The particle size, and particle size distribution of SPIONs were measured with a malvern instrument. The particle size distribution is reported as poly dispersity index. The samples were placed in the analyzer chamber and readings were performed at 25°C with a detected angle of 90 degrees. The zeta potential of SPIONs was measured with a malvern instrument (Zetasizer 3000 HS U.K). The samples were diluted and placed in electrophoretic cell and measured in the automatic mode[7].

Determination of Zeta Potential

Zeta potential is a measure of surface charge. The surface charge (electrophoretic mobility) of nanoparticle can be determined by using Zeta sizer (Malvern Instrument) having zeta cells, polycarbonate cell with gold plated electrodes and using water as medium for sample preparation. It is essential for the characterisation of stability of the nanoparticle[7].

Drug loading efficiency

The encapsulation efficiency and loading capacity of SPIONs were determined by the separation of SPIONs from the supernatant liquid containing non associated silymarin obtained after cold centrifugation at 12000g for 30 minutes. The amount of free silymarin in the supernatant liquid was measured by UV-Vis Spectrophotometer at 288nm. The experiment was run in triplicate using 7.4 phosphate buffer and the mean values were recorded. The silymarin encapsulation efficiency (EE) of the SPIONs was calculated from the following equations[30].

The amount of entrapped drug is calculated from the equation.

$$\%\ Drug\ Entrpment = \frac{Total\ amount\ of\ drug - free\ drug}{Total\ amount\ of\ drug} \times 100$$

Drug release study

The drug release behaviour of nanoparticles was studied in physiological pH of 7.4 and acidic media with the pH of 5.3 in phosphate-buffered saline, PBS containing 0.5% (w/v) Tween 80. Typically, 10mg of nanoparticles were placed into a dialysis bag (cut off 12kDa) and introduced to 15 mL of PBS with desired pH under stirring (100 rpm) at 37 °C. At predetermined time intervals, in order to determine the drug concentration in dialysate and thereby time-dependent drug release profile, 1.0 mL of dialysate was taken out and replaced with 1.0mL of fresh buffer solution maintained at 37 °C and assayed by UV–Vis spectroscopy at wavelength of 288 nm[30].

Results & Discussion

RESULTS AND DISCUSSION

PREFORMULATION STUDIES

Physical Characteristics

Silymarin was checked for its colour, odour, and texture. Silymarin is light yellow coloured powder in appearance, odourless and amorphous in nature.

Solubility

Solubility test for Silymarin was carried out in different solvents such as ethanol, water, dichloromethane and chloroform and results are given in Table 3.

Table 3: Solubility test for Silymarin in different solvents

Sl. No	Solvent	Soluble	Sparing Soluble	Insoluble
1.	Ethanol	✓	-	-
2.	Dichloromethane	✓	-	-
3.	Chloroform	-…	✓	-
4.	Water	-	-	✓

Selection of Wavelength

The Silymarin stock solution of concentration 100 µg/mL was scanned in the range of 200-400nm for λmax. using double beam UV Spectrophotometer. The absorption peak obtained is shown in Figure 1.

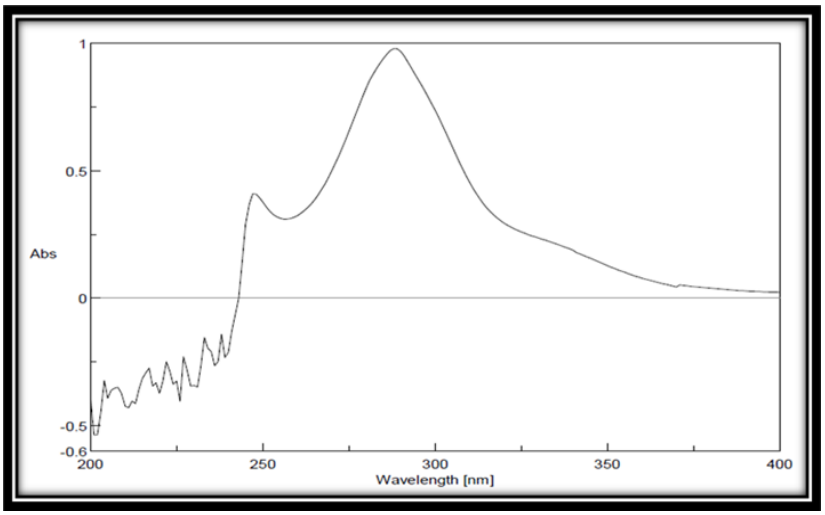

Figure 1: UV spectrum of silymarin.

The maximum absorption of Silymarin was found to be at 288 nm and hence it is selected as the wavelength for further studies.

Construction of calibration curve of Silymarin

In the buffer solution pH 6.8 solution, linearity was obtained between 5-40 µg/ml concentration of Silymarin and the regression value was found to be r^2 = 0.9996. Hence, we can conclude that Silymarin obeys Beer Lambert's Law at the concentration between 5-40 µg/ml. The results are shown in Table 4 represents the concentration and absorbance value of silymarin in the buffer solution pH 6.8 and Figure 2 represents the calibration curve of silymarin.

Table 4: Concentration and absorbance values for the calibration curve of Silymarin at 288nm (pH 6.8)

Sl. No	Concentration (µg/ml)	Absorbance at 288nm
1	1	0.0595
2	2	0.1144
3	3	0.1667
4	4	0.2201
5	5	0.2711

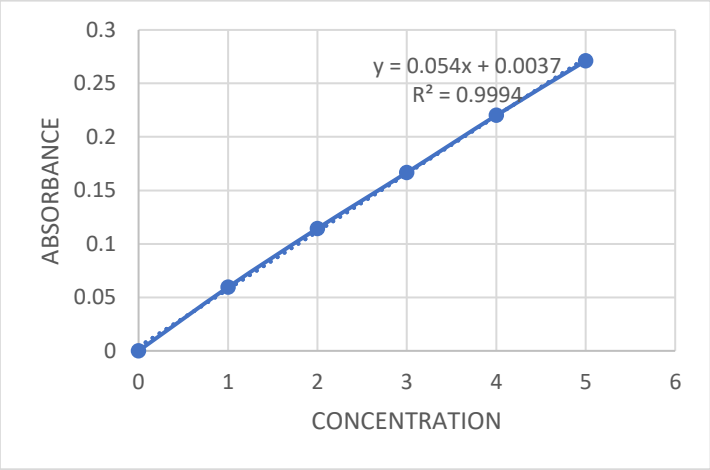

Figure 2: Calibration curve of silymarin

MOLECULAR DOCKING STUDY

Molecular docking analysis performed to evaluate the most preferred geometry of the protein ligand complex. Docking phase is meaningless without its two components such as target protein and ligand. Homosapien covid receptors were used for performing docking study as target proteins. Docking results identify native or native-like configurations of the protein-ligand complex.

Silymarin can also be an affective compound in the treatment of COVID-19. Its binding affinity with covid receptors is evaluated by using docking studies and further silymarin is compared with the most potent currently used drug remdesivir for covid 19 treatment. Silymarin was successfully docked with the covid receptor proteins. The binding affinities of silymarin to the target proteins are denoted in the table 5 below;

Table 5: Binding affinity of Silymarin with the covid receptors.

Sl. No	Receptor	Binding affinity
1.	7JMP	-7.23
2.	5N11	-8.09
3.	7JMO	-6.96
4.	4RNA	-5.25
5.	6VYB	-5.32
6.	6LU7	-6.55
7.	7LMF	-5.79
8.	6VXX	-6.31
9.	7LMF	-5.79

Among these receptors the having dock score of −5 or more are considered to have better binding affinity for the COVID-19. The binding affinity data in Table 5. shows, the code of 5N11, 7JMP, 7JMO, 6LU7, and 6VXX covid receptors shows the binding affinities of -8.09, -7.23, -6.96, -6.55 and -6.31 respectively have higher the docking score than -5 and are further considered for the study. In spite of the good binding ability of receptors 6LU7 and 6VXX with docking score of more than -5, they are not selected for the study as only three receptors

with high affinity are considered for further analysis. Hence, the receptors code of 5N11, 7JMP and 7JMO with high binding affinity than other receptors are selected for further study which is further compared with the standard Remdesivir and the results are shown in Table 6.

Table 6: Binding affinity of Remdesivir with the covid receptors.

Receptor	Binding affinity towards Remdesivir	Binding affinity towards silymarin
5N11	-5.21	-8.09
7JMP	-3.76	-7.23
7JMO	-2.97	-6.96

From table it is known that the binding affinity of these receptor 5N11, 7JMP, 7JMO have higher docking score for silymarin than with the standard Remdesivir (-8.09>-5.21>, -7.23>-3.76, -6.96>-2.97) respectively. By the comparative analysis study, it is understood that silymarin has the highest docking score value and has high binding affinity towards the covid receptors compared to the Remdesivir.

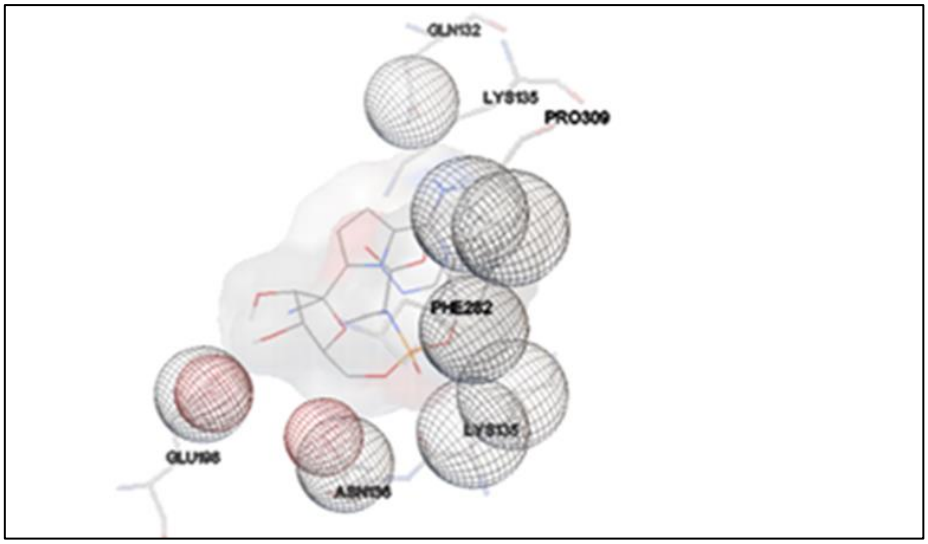

Figure 3: Potential binding sites of 5N11 receptor with Remdesivir

The fig 3 represents the various amino acid binding sites of 5N11 with Remdesivir (GLN-Glutamine, LYS-Lysine, PRO-Proline, PHE-Phenylalanine, ASN-Asparagine, GLU-Glutamic acid)

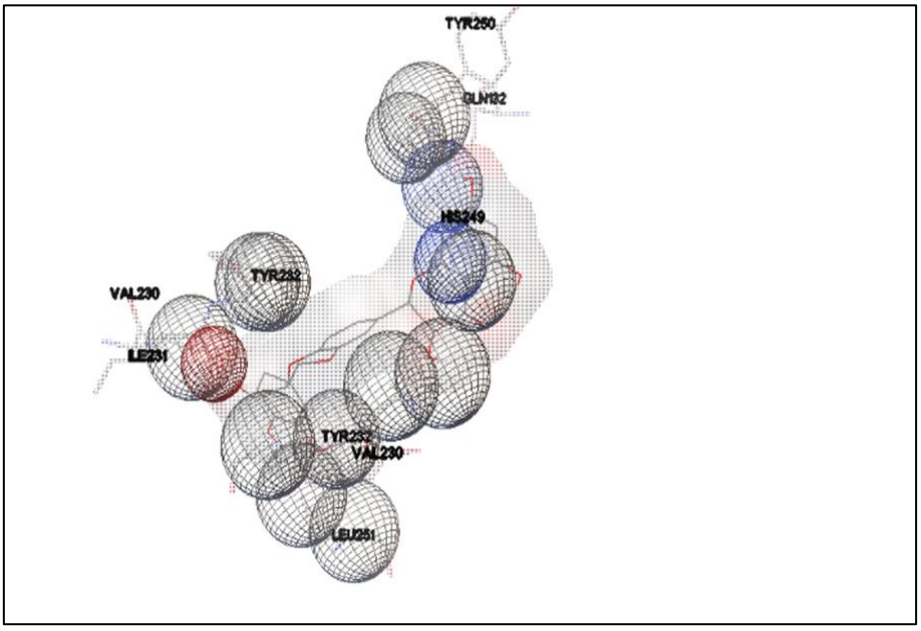

Figure 4: Potential binding sites of 5N11receptor with silymarin

The fig 4 represents the various amino acid binding sites of 5N11 with Silymarin (TYR-Tyrosine, GLN-Glutamine, VAL-Valine, LEU-Leucine, HIS-Histidine, ILE-Isoleucine)

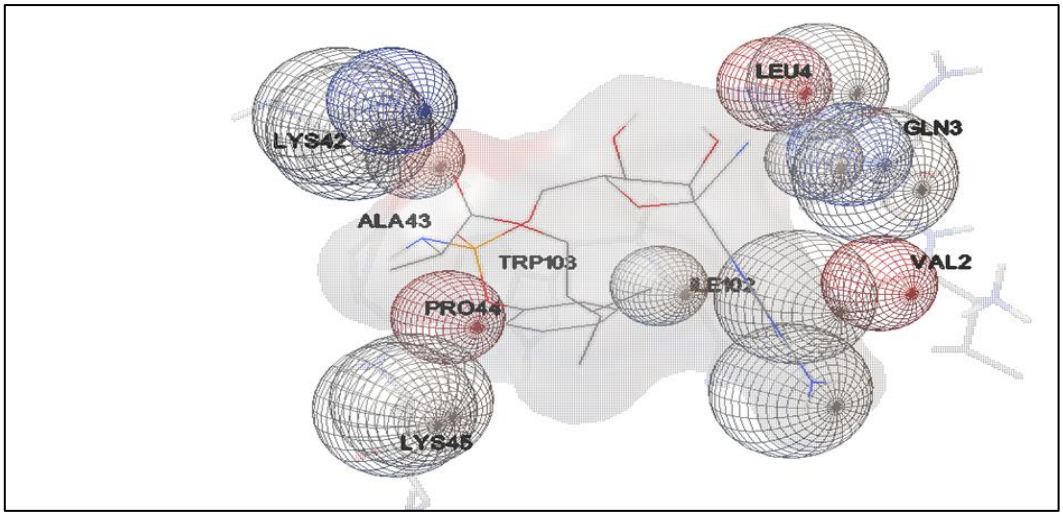

Figure 5: Potential binding sites of 7JMP receptor with Remdesivir

The fig 5 represents the various amino acid binding sites of 7JMP with Remdesivir (LEU-Leucine, GLN-Glutamine, VAL-Valine, ILE-Isoleucine, TRP-Tryptophan, LYS-Lysine, ALA-Alanine, PRO-Proline)

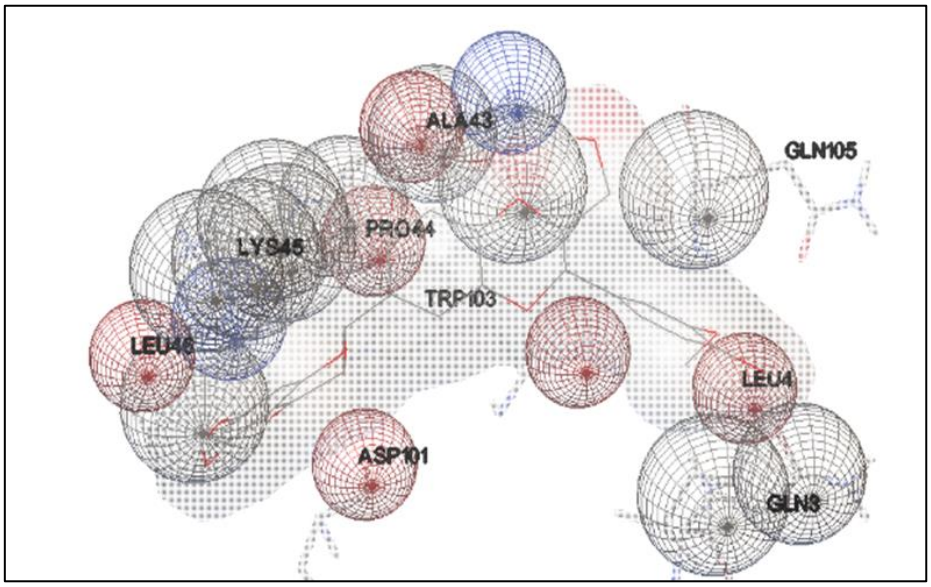

Figure 6: Potential binding sites of 7JMP receptor with Silymarin

The fig 6 represents the various amino acid binding sites of 7JMP with Silymarin (ALA-Alanine, GLN-Glutamine, PRO-Proline, LYS-Lysine, TRP-Tryptophan, LEU-Leucine, ASP-Aspartic acid)

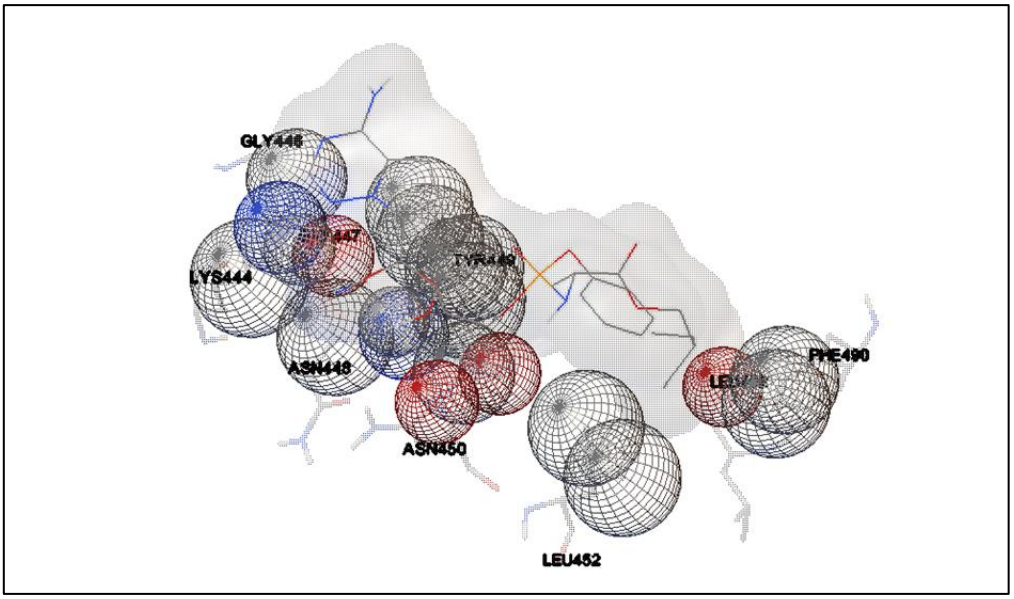

Figure 7: Potential binding sites of 7JMO receptor with Remdesivir

The fig 7 represents the various amino acid binding sites of 7JMO with Remdesivir (GLY-Glycine, LEU-Leucine, PHE-Phenylalanine, ASN-Asparagine, LYS-Lysine)

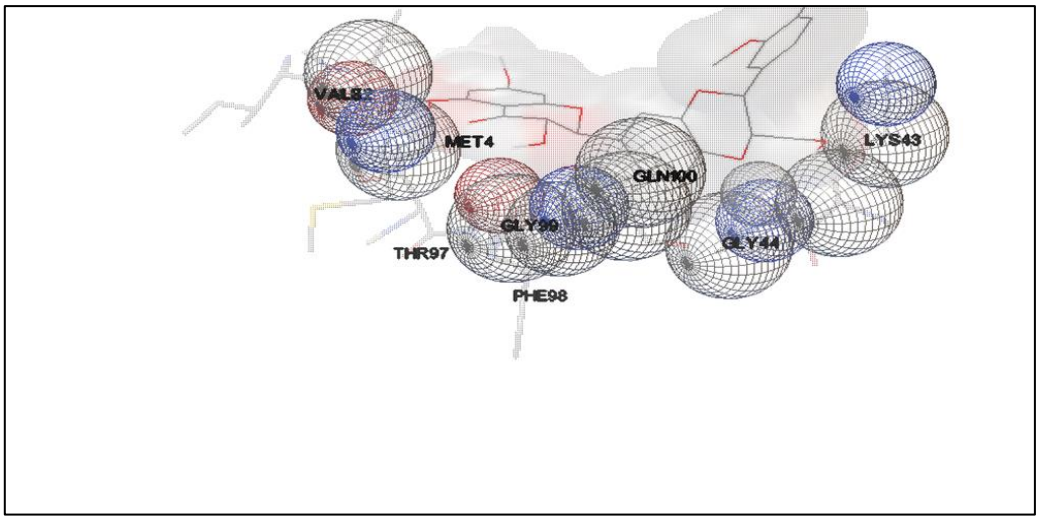

Figure 8: Potential binding sites of 7JMO receptor with silymarin

The fig 8 represents the various amino acid binding sites of 7JMO with Silymarin (VAL-Valine, MET-Methionine, THR-Threonine, PHE-Phenylalanine, GLN-Glutamine, GLY-Glycine, LYS-Lysine)

The potential binding sites of Remdesivir with 5N11, 7JMP and 7JMO receptor are shown in Figure 3, Figure 5, and Figure 7 respectively and the potential binding sites of Silymarin with 5N11, 7JMP and 7JMO receptor are shown in Figure 4, Figure 6 and Figure 8 respectively. The possible binding modes of these receptor have active sites which has been shown in Table 7, the protein residues with silymarin and Remdesivir ligand molecule are shown in Table 7.

Table 7: Binding interaction with amnio acid residue of silymarin and Remdesivir

Receptor	Silymarin	Remdesivir
5N11	TYR250, GLN132, TYR232, VAL230, LEU251, TYR282, LE231, HIS249, ILE231	GLN132, LYS135, PRO309, PHE282, LYS135, ASN136, GLU198
7JMP	ALA43, GLN105, PRO44, LYS45, TRP103, LEU46, ASP101, LEU4, GLN3	LEU4, GLN3, VAL2, LE102, TRP103, LYS42, ALA43, PRO44, LYS45
7JMO	VAL62, MET4, THR97, GLY99, PHE98, GLN100, GLY44, LYS43	GLY446, LEU452, PHE490, ASN450, ASN448, LYS444

The possible binding modes of 5N11 receptor having active sites to which the silymarin binds to this amino acid are TYR250, LN132, TYR232, VAL230, LEU251, TYR282, LE231, MS249 while with Remdesivir the protein residues are LN132, LYS135, PRO309, PHE282, LYS135, ASN136, GLU198.The binding modes of 7JMP receptor having active sites ALA43, GLN105, PRO44, LYS45, TRP103, LEU46, ASP101, LEU4, GLN3 with silymarin and the Remdesivir have the protein residues as LEU4, GLN3, VAL2, LE102, TRP103, LYS42, ALA43, PRO44, LYS45. And for the receptor 7JMO the binding modes with silymarin, the protein residue is VAL62, MET4, THR97, GLY99, PHE98, GLN100, GLY44, LYS43 and the protein residue GLY446, LEU452, PHE490, ASN450, ASN448, LYS444 is the binding mode for Remdesivir.

In this study, studies were performed over binding pocket of COVID-19 to find the potential small molecule docking to combat life threatening corona virus diseases. The study finds that by comparative analysis the docking score of silymarin ligand is higher than the Remdesivir and has better binding affinity than Remdesivir. therefore, silymarin will act as better agent of drug for the treatment of covid 19. As the antiviral activity of silymarin which has been reported for various other viruses, this can also act as n better anti-viral agent for the better treatment of covid 19 due to its high binding ability.

So Silymarin magnetic nanoparticle could be an affective compound in the treatment of COVID-19 as it can act as a targeting agent at the particular site of affected lungs where it can affectedly target the covid receptors for a better treatment.

FORMULATION OF MAGNETIC NANOPARTICLE

Silymarin magnetic nanoparticle were prepared by co- precipitation method and further polymers and drug were encapsulated by Double emulsion method. Various trial batches were carried out using different polymers with different concentration such as eudragit, ethyl cellulose and polyethylene glycol which is represented in Table 8. Ferric chloride and Ferrous chloride were added as iron source to the formulation for magnetic property. The magnetic nanoparticle were prepared by the use of probe sonicator. The sonication time also varied for the formulation.

Co-precipitation is one of the most popular procedures to formulate SPIONs, that has been widely used. The black precipitate is obtained at the end of every formulation. This is due to the addition of base to an aqueous solution of Fe^{2+} and Fe^{3+} ions in a 1:2 stoichiometry ratio. The magnetization of the prepared nanoparticle is based on the magnetic moments of its magnetic constituents Fe^{2+} and Fe^{3+}. This magnetic field of the nanoparticle reveals the magnetic interaction modes at a microscopic molecular level.

Table 8: formulation of silymarin nanoparticle with various polymer concentration

Sl.NO	Ingredient	F1	F2	F3	F4	F5	F6	F7	F8	F9	F10	F11	F12
1.	Silymarin (mg)	10	10	10	10	10	10	10	10	10	10	10	10
2.	Ferric chloride(mg)	0.48	0.48	0.48	0.48	0.48	0.48	0.48	0.48	0.48	0.48	0.48	0.48
3.	Ferrous chloride(mg)	0.19	0.19	0.19	0.19	0.19	0.19	0.19	0.19	0.19	0.19	0.19	0.19
4.	Silymarin:eudragit	1:1	1:1	1:2	1:2	1:1	1:1	1:2	1:2	1:1	1:1	1:2	1:2
5.	Silymarin:ethyl cellulose	1:1	1:1	1:2	1:2	1:1	1:1	1:2	1:2	1:1	1:1	1:2	1:2
6.	Silymarin: poly ethylene glycol	1:1	1:1	1:2	1:2	1:1	1:1	1:2	1:2	1:1	1:1	1:2	1:2
7.	Sonication time In hours	1	1	3	3	1	1	3	3	1	1	3	3

Percentage yield

The percentage yield of the formulated Silymarin magnetic nanoparticle were given in the Table 9. The percentage yield is low in formulation F1,F2,F3 and F4 ie, below 30% and high in formulation F5, F6, F7 and F8 (78.16 %). It can also be noted that the yield obtained while using ethyl cellulose as polymer is much higher when compared with eudragit and polyethylene glycol. The percentage yield analysis of all formulations is depicted in table 9. Since the yield is less in formulations F1-F5 with Eudragit, they are not considered for further studies.

Table 9: Percentage yield analysis of different formulation

S. No	Formulation code	Percentage yield (%)
1.	F1	34.14
2.	F2	32.14
3.	F3	30.14
4.	F4	29.14
5.	F5	71.25
6.	F6	75.16
7.	F7	73.25
8.	F8	78.16
9.	F9	50.13
10.	F10	55.25
11.	F11	53.13
12.	F12	57.25

Particle Size and Entrapment efficiency

The particle size is one of the most important parameters for the characterisation of nanoparticle. The average particle sizes of the prepared Silymarin magnetic nanoparticle were measured using Malvern zeta sizer.

Table 10: Particle size and entrapment efficiency of formulation

S. No	Formulation code	Particle size nm	Entrapment Efficiency (%)
1.	F5	1924	93.2
2.	F6	724	94.43
3.	F7	928	91.2
4.	F8	319	96.43
5.	F9	1941	82.15
6.	F10	638	83.09
7	F11	728	80.15
8	F12	538	84.09

The table 10 indicated that the sonication time increased from 1 hour to 3 hour, the small size nanoparticle are obtained. This may be due to the increased sonication energy which reduces particle size of nanoparticle. Particle size analysis showed that the average particle size of Silymarin magnetic nanoparticle (F8) formulated using 1:2 ratio of ethyl cellulose was found to be 319 nm with polydispersity index (PDI) value 0.636 and with intercept 0.939. The zeta size distribution of ethyl cellulose silymarin magnetic nanoparticle is depicted in Figure 9.

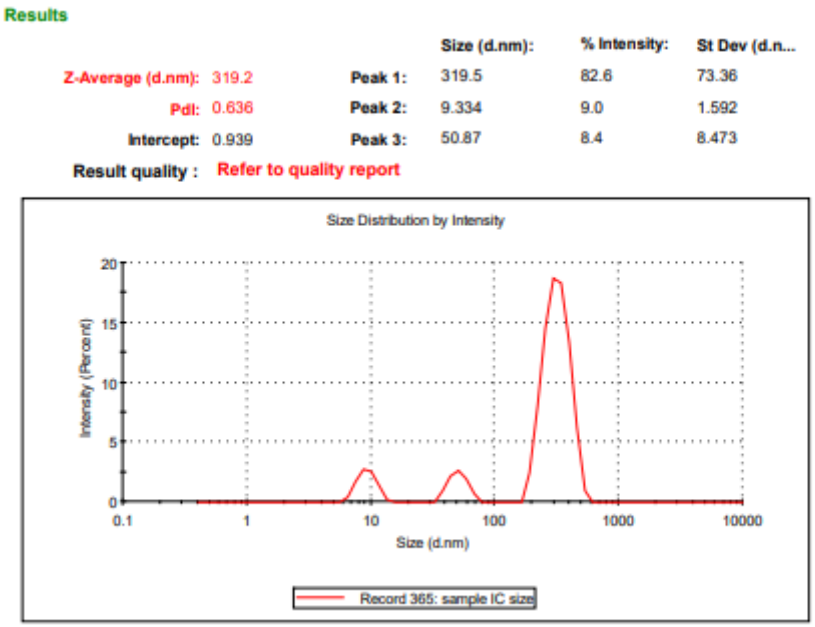

Figure 9: Zeta size distribution of Silymarin magnetic nanoparticle with ethyl cellulose

Particle size analysis showed that the average particle size of Silymarin magnetic nanoparticle (F9) formulated using 1:1 ratio of polyethylene glycol was found to be 1941 nm with polydispersity index (PDI) value 0.320 and with intercept 0.850. The zeta size distribution of poly ethylene glycol silymarin magnetic nanoparticle is depicted in Figure 10.

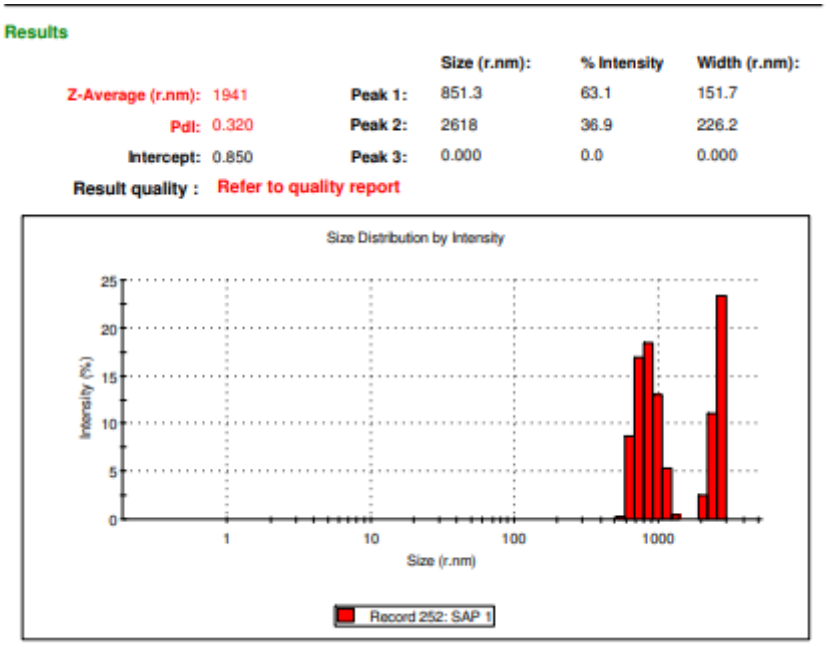

Figure 10: Zeta size distribution of Silymarin magnetic nanoparticle with poly ethylene glycol.

The prepared magnetic nanoparticle particle possesses high drug entrapment efficiency and were found to be in the range of 82.15% - 96.43%. The variation in entrapment efficiency was due to the changes in the polymer concentration and difference in degree of cross linking (Vidya *et al.*2015). The entrapment efficiency was found to be highest for F8 formulation (Silymarin: ethyl cellulose, ratio 1:2) which is 96.43% and the lowest entrapment of drug was found for F11 formulation (Silymarin: polyethylene glycol ratio 1:2) which is 80.15%**.**

Since the entrapment efficiency is high 96.43% and particle size is less 319 nm for formulation F8 among other formulation, it is considered for Zeta potential measurement and SEM analysis.

Determination of Zeta Potential

Zeta Potential was determined using Malvern zeta-sizer instrument. Zeta potential analysis is carried out to find the surface charge of the particles to know its stability during storage. The magnitude of zeta potential is predictive of the colloidal stability. Nanoparticles with zeta potential value greater than +25 mV or less than -25 mV typically have high degrees of stability. If all the particles in suspension have a large negative or positive zeta potential then they will tend to repel each other and there will be no tendency for the particles to come together. However, if the particles have low zeta potential value, then there will be no force to prevent the particles coming together and flocculating. For Silymarin magnetic nanoparticle using ethyl cellulose zeta potential was found to be -9.68 mV with peak area of 100% intensity. These values indicate that the formulated Silymarin magnetic nanoparticle are stable. Zeta potential distribution of Silymarin magnetic nanoparticle prepared using ethyl cellulose F8 is depicted in the Figure 11

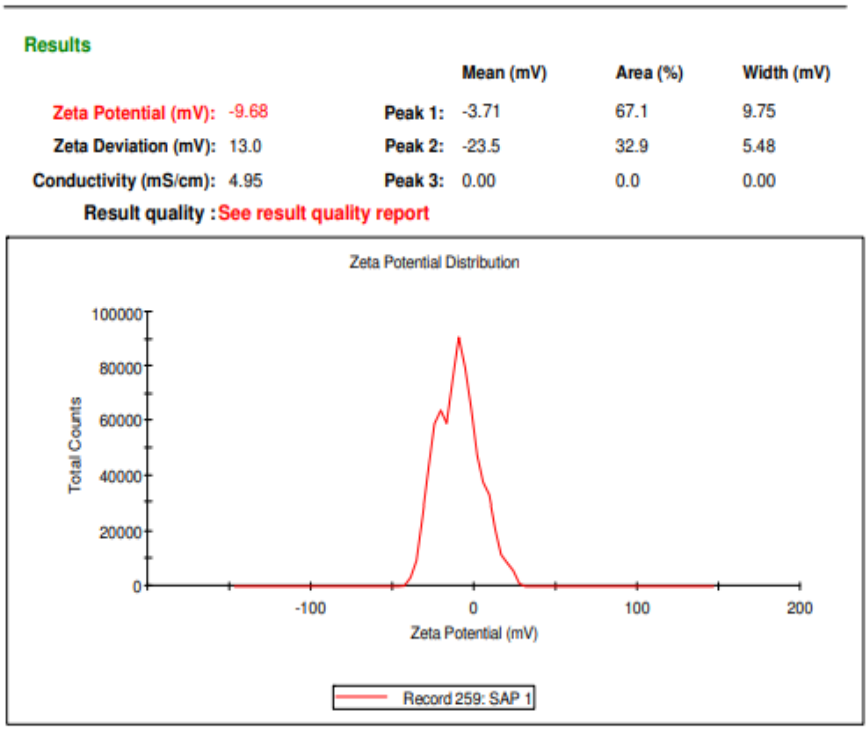

Figure 11: Zeta potential of Silymarin magnetic nanoparticle

Scanning Electron Microscopy

SEM analyses of the formulated Silymarin magnetic nanoparticle were performed to evaluate the surface morphology of magnetic nanoparticle.

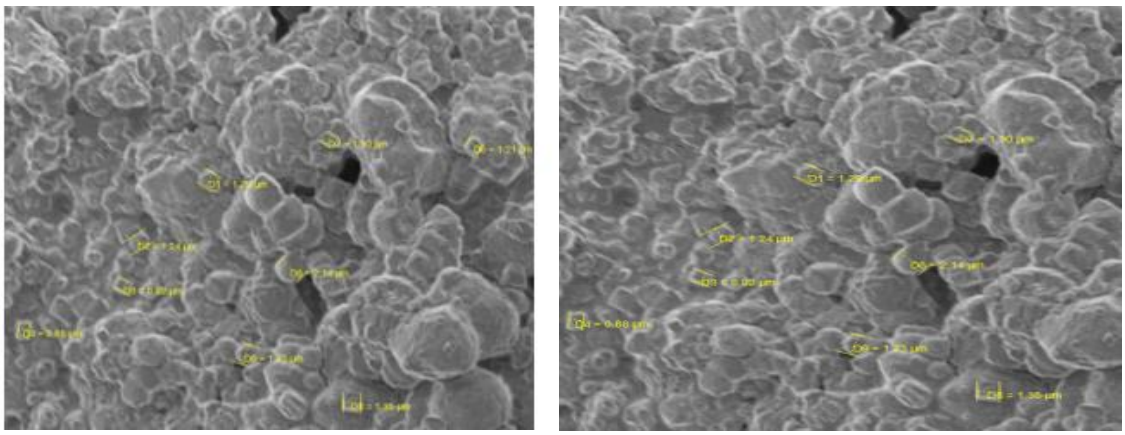

Figure 12: Scanning electron microscopy of silymarin entrapped SPION'S

The morphology of prepared silymarin entrapped SPIONs F4 is obtained by SEM and it is shown in Figure 12. The Figure 12 represent that the SPIONs prepared are poly dispersed and spherical in shape.

FTIR Spectroscopy of Silymarin magnetic nanoparticle

Fourier Transform Infrared (FT-IR) spectra of the samples were obtained using a FTIR Jasco 4100 Spectrometer by KBr pellet method. The spectrums of pure drug (Silymarin), ethyl cellulose, Eudragit and poly ethylene glycol and the formulation of silymarin magnetic nanoparticle with respective polymers are shown in figure 13,14, 15 ,16, 17,18 and 19 and their interpretation are given in table 11,12,13,14,15,16 and 17 below respectively.

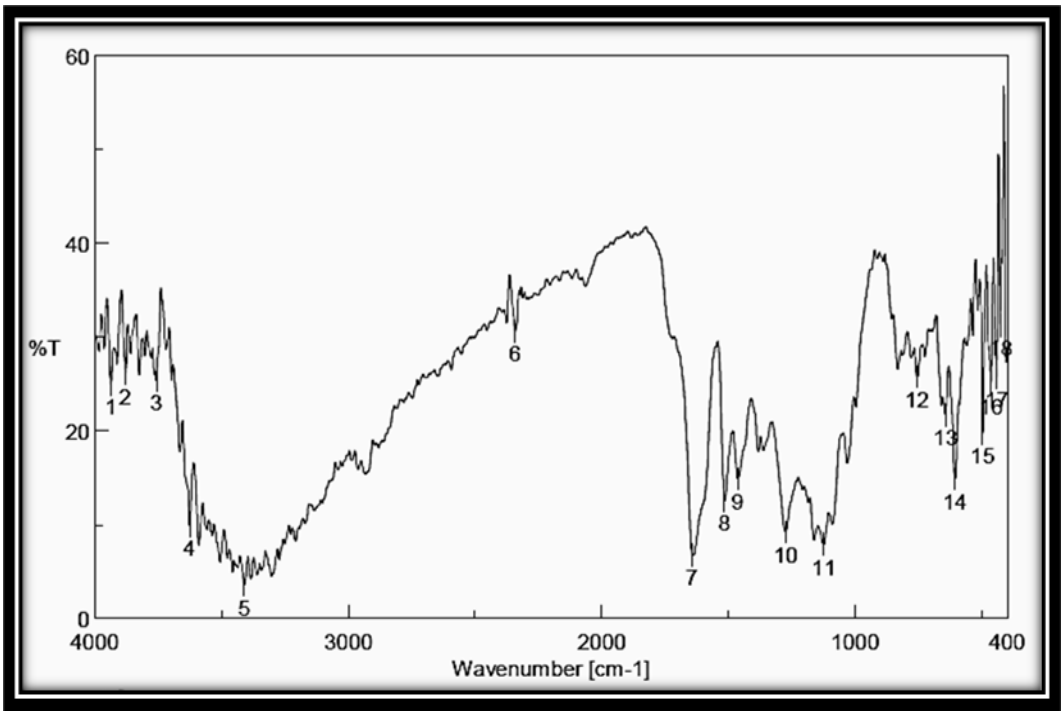

Figure 13: FTIR spectrum of Silymarin

Table 11: FTIR interpretation of Silymarin

Materials	Standard wave number (cm^{-1})	Test wave number (cm^{-1})	Functional group assignment
SILYMARIN	3650-3200	3410.49 3625.52	OH stretching
	1820-1665	1643.05	C=O stretching
	1320-1210	1273.75	C-O-C stretching
	1161-1029	1121.4	In plane =C-H bending

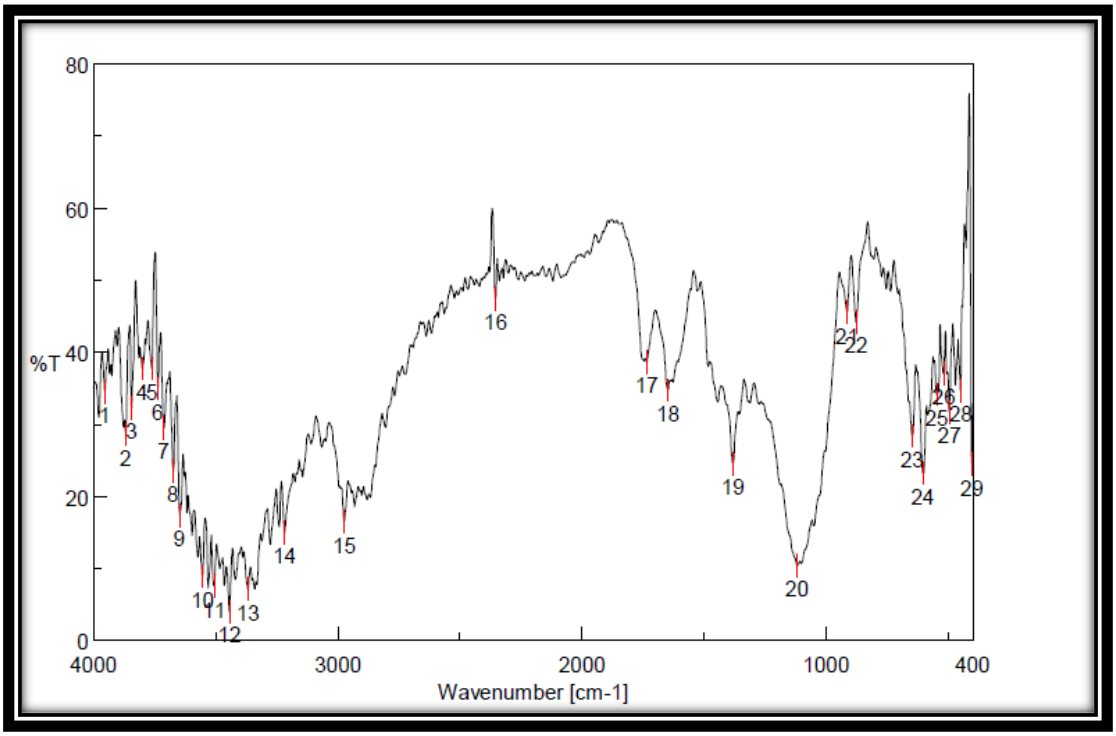

Figure 14: FTIR spectrum of Ethyl Cellulose

Table 12: FTIR interpretation of Ethyl Cellulose

Materials	Standard wave number (cm^{-1})	Test wave number (cm^{-1})	Functional group assignment
ETHYL CELLULOSE	3650-3200	3647.7	O-H stretching
	2960-2850	2974.66	C-H stretching
	1820-1665	1734.66	C=O stretching
	1680-1620	1647.88	C=C stretching
	1300-1000	1118.51	C-O stretching

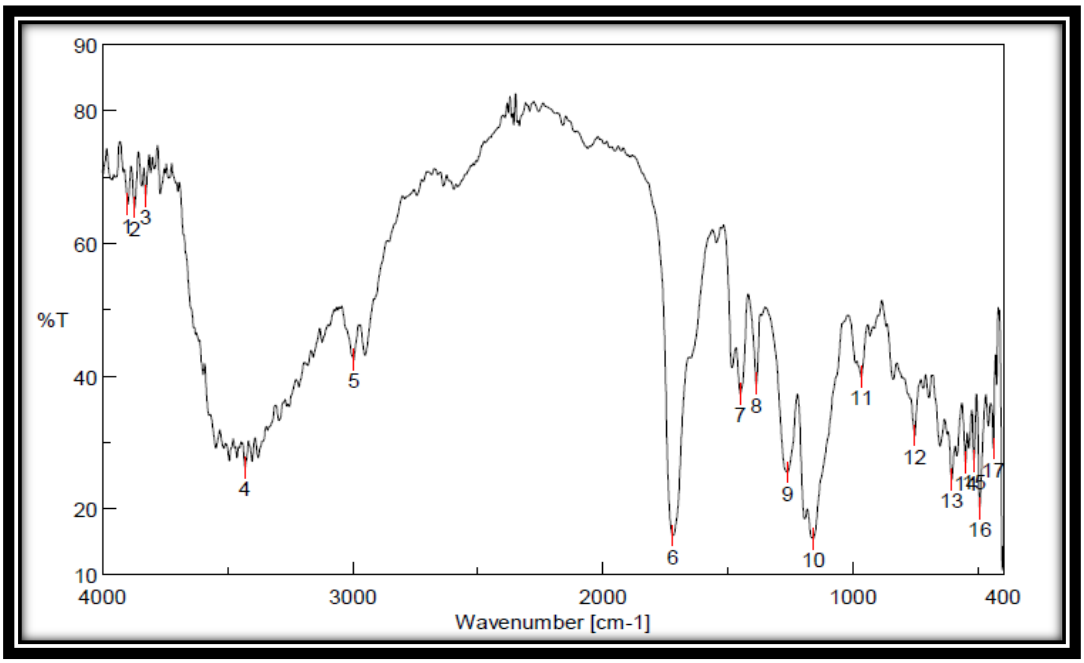

Figure 15: FTIR spectrum of Eudragit

Table 13: FTIR interpretation of Eudragit

Materials	Standard wave number (cm^{-1})	Test wave number (cm^{-1})	Functional group assignment
EUDRAGIT	3000-3700	3430.74	O-H stretching
	1500-1800	1720.19	N-H bending
	2700-3300	2995.87	C-H stretching
	1300-1500	1451.17 1386.57	C-H bending
	1000-1300	1262.18 1159.01	C-O stretching

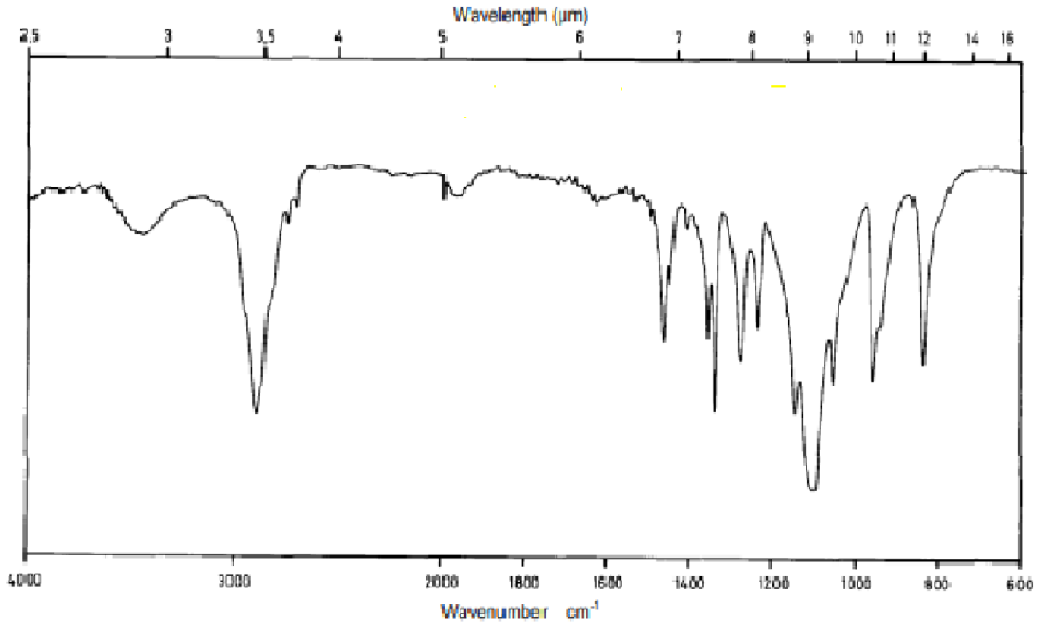

Figure 16: FTIR spectrum of poly ethylene glycol

Table 14: FTIR interpretation of polyethylene glycol

Materials	Standard wave number (cm^{-1})	Test wave number (cm^{-1})	Functional group assignment
POLYETHYLENE GLYCOL	3000-3700	3430.74	O-H stretching
	1500-1800	1720.19	N-H bending
	2700-3300	2995.87	C-H stretching
	1300-1500	1451.17 1386.57	C-H bending
	1000-1300	1262.18 1159.01	C-O stretching

FTIR spectrum of Silymarin magnetic nanoparticle using ethyl cellulose is given in Figure 17.

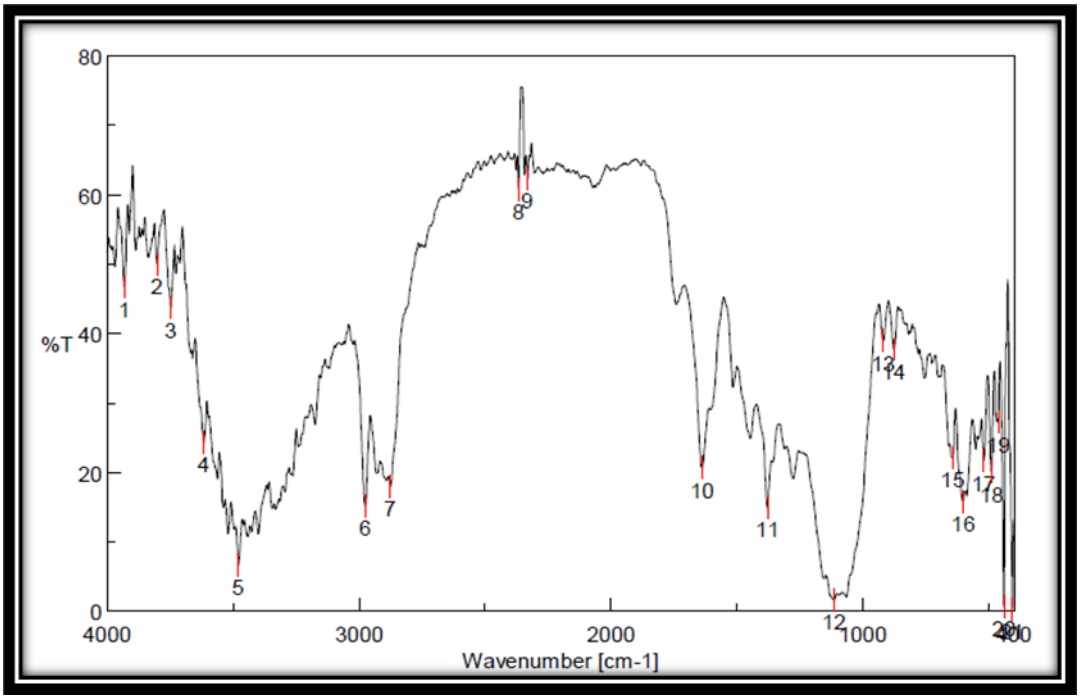

Figure 17: FTIR spectrum of Silymarin magnetic nanoparticle using EC

Table 15: FTIR interpretation of Silymarin magnetic nanoparticle using EC

Materials	Standard wave number (cm^{-1})	Test wave number (cm^{-1})	Functional group assignment
FORMULATION OF SILYMARIN WITH ETHYL CELLULOSE	3650-3200	3615.88 3478.95	OH stretching
	2970-2850	2876.31	C-H stretching
	1725-1665	1668.23	C=O stretching
	1161-1029	1114.65	In plane =C-H bending
	800-600	876.488 643.144	C-H rocking

FTIR spectrum of Silymarin magnetic nanoparticle using eudragit is given in Figure 18.

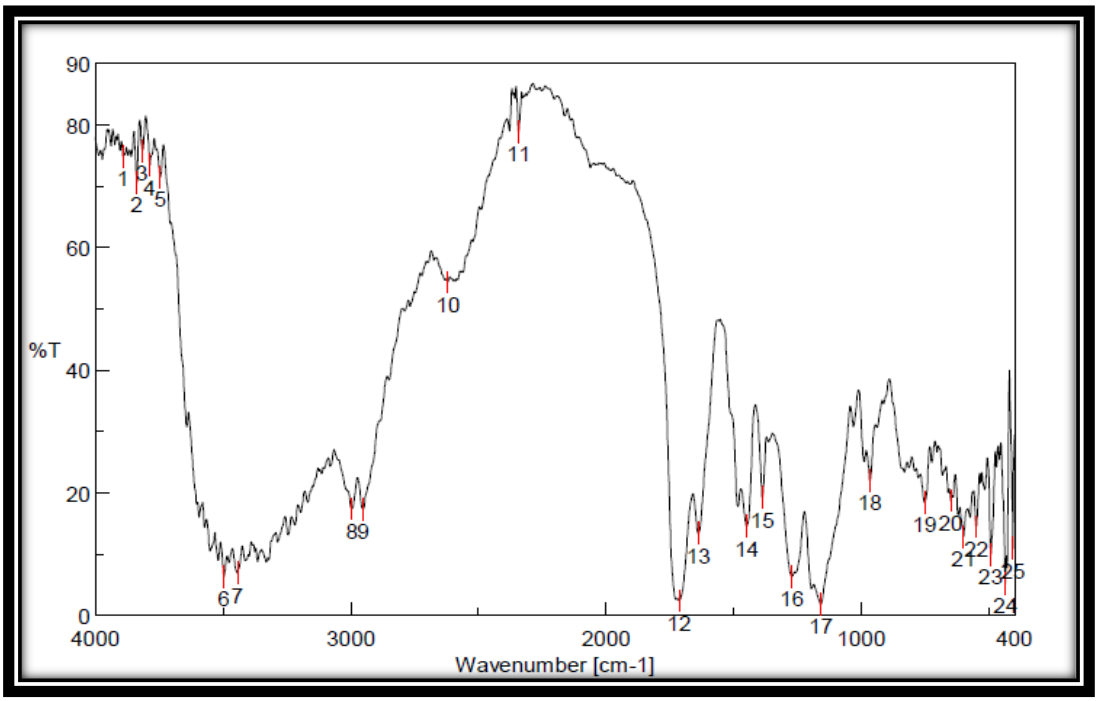

Figure 18: FTIR spectrum of Silymarin magnetic nanoparticle using Eudragit

Table 16: FTIR interpretation of Silymarin magnetic nanoparticle using Eudragit

Materials	**Standard wave number (cm^{-1})**	**Test wave number (cm^{-1})**	**Functional group assignment**
FORMULATION OF SILYMARIN WITH EUDRAGIT	3650-3200	3497.27 3444.24	OH stretching
	3300-2700	2993.94 2951.52	C-H stretching
	1820-1665	1714.41	C=O stretching
	1800-1500	1638.23	N-H bending
	1500-1300	1449.24	C-H bending
	1320-1210	1271.82	C-O-C stretching
	1161-1029	1159.01	In plane =C-H bending
	800-600	753.066 648.929	C-H rocking

FTIR spectrum of Silymarin magnetic nanoparticle using poly ethylene glycol is given in Figure 19.

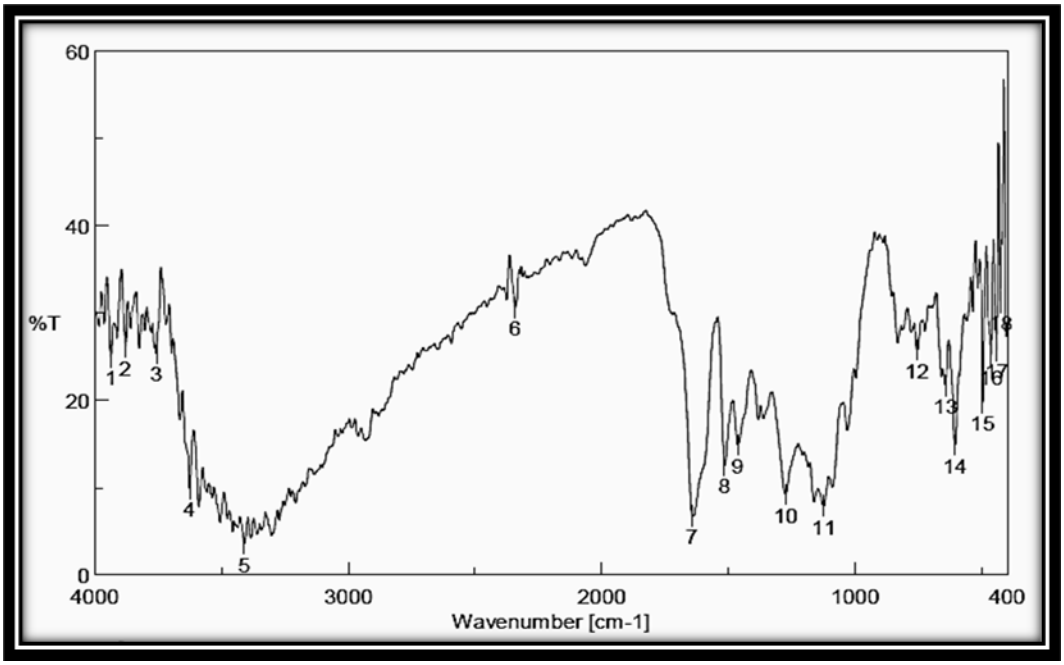

Figure 19: FTIR spectrum of Silymarin magnetic nanoparticle using PEG

Table 17: FTIR interpretation of Silymarin magnetic nanoparticle using poly ethylene glycol

Materials	Standard wave number (cm^{-1})	Test wave number (cm^{-1})	Functional group assignment
FORMULATION OF SILYMARIN WITH POLYETHLENE GLCOL	3650-3200	3410.49 3625.52	OH stretching
	1820-1665	1643.05	C=O stretching
	1320-1210	1273.75	C-O-C stretching
	1161-1029	1121.4	In plane =C-H bending

The peaks present in the FTIR spectra of pure Silymarin are present in the FTIR spectra of all the above formulation. The main peaks such as OH stretching, C=O stretching and in plane

=C-H bending are present in the formulation, so we conclude that drug and polymer are compatible.

IN-VITRO DRUG RELEASE STUDIES

In vitro drug release study of the prepared Silymarin magnetic nanoparticle was carried out using dialysis bag diffusion method. Amount of drug released in different time intervals were observed.

In vitro drug release profile data obtained for the formulation of Silymarin magnetic nanoparticle with ethyl cellulose, polyethylene glycol is given in Table 18.

Table 18: *In-vitro* drug release profile of Silymarin magnetic nanoparticle

Sl. No	Time (hrs)	Cumulative percentage drug released (%)							
		F5	F6	F7	F8	F9	F10	F11	F12
1	0	0	0	0	0	0	0	0	0
2	1	11.37	10.37	10.65	6.46	3.408	5.408	5.11	5.11
3	2	18.94	16.24	10.37	11.47	10.78	14.58	9.82	11.82
4	4	30.28	24.32	19.76	17.23	25.46	23.46	26.65	24.23
5	8	66.56	58.32	44.58	45.58	52.56	57.46	47.38	46.28
6	12	86.07	82.27	60.19	64.19	65.46	63.46	67.39	69.59
7	24	111.26	98.26	91.12	94.12	98.78	99.78	99.31	97.71

In-vitro drug release data indicates that both hydrophobic polymer ethyl cellulose and poly ethylene glycol have sustained the release of drug. There is no significant effect in polymer type. Drug release was observed as a function of drug: polymer ratio type. It was observed that the drug release decreased with the increase in the amount of polymer for each formulation of ethyl cellulose and polyethylene glycol. This is due to the drug release is retarded with the difficulty of the drug to diffuse in the increased swollen matrix of the polymer with the higher concentration.

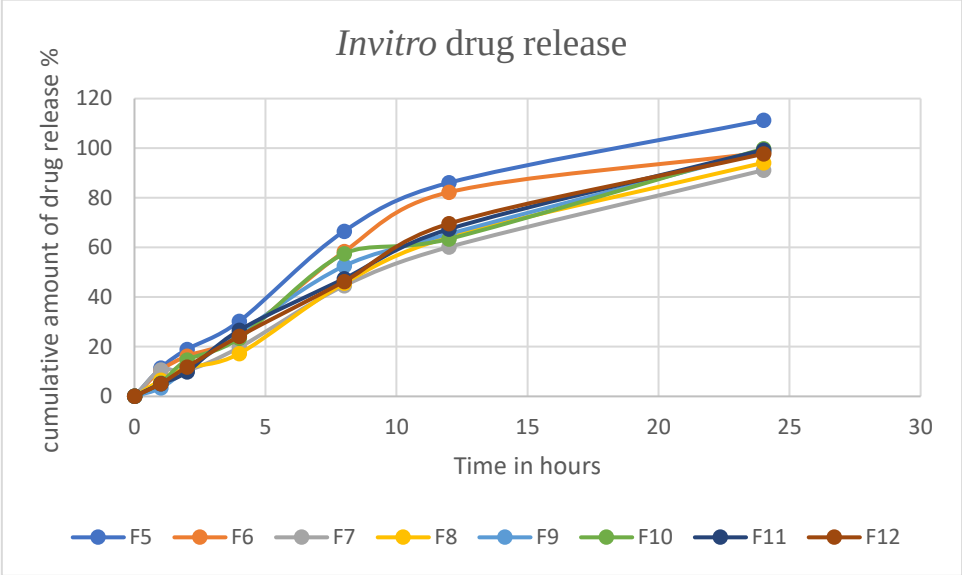

Figure 20. Invitro drug release of formulation

So the formulation F8 with the drug release 94.12% at the end of 24 hours is considered as optimized formulation.

IN-VITRO DRUG RELEASE KINETICS

The data obtained from the *in vitro* release study was used for kinetic modelling. This was done to find out the mechanism of drug release from Silymarin magnetic nanoparticle. In order to determine the release model, the *in vitro* release data were analysed according to zero order, first order and diffusion-controlled mechanism according to simplified Higuchi model. The preference of a certain mechanism was based on the coefficient of determination (r^2) for the parameters studied, where the highest coefficient of determination is preferred for the selection of the order of release. The data is presented in Table 19 and graph represented for respective formulation in figure 23,24,25,26,27 and 28.

The *in vitro* release model best fitted to Higuchi release order. This was confirmed by plotting percentage cumulative drug release and square root of time and r^2 value ranges between 0.8477 and 0.9888. However, in many experimental situations, the mechanism of drug diffusion deviates from the Fickian equation and follows a non-Fickian (anomalous) behaviour. In these cases, the Korsemeyer–Peppas model was used to analyse the release kinetics. It is observed that all the formulation F5 - F12 followed Non - Fick's law of diffusion.

Table 19: Kinetic parameters of the release data of Silymarin magnetic nanoparticle

Formulation	r^2			Mechanism	Korsemeyer-Peppas Model		
	Zero	First	Higuchi		r^2	n	Mechanism
F5	0.7348	0.9871	0.9079	Diffusion	0.7795	0.677	Non fickian
F6	0.7348	0.9826	0.9079	Diffusion	0.7795	0.5813	Non fickian
F7	0.7348	0.980	0.9079	Diffusion	0.7795	0.9302	Non fickian
F8	0.7348	0.9734	0.9079	Diffusion	0.7795	0.5847	Non fickian
F9	0.7348	0.9296	0.9079	Diffusion	0.7795	0.8431	Non fickian
F10	0.7348	0.8849	0.9079	Diffusion	0.7795	0.6843	Non fickian
F11	0.7348	0.9135	0.9079	Diffusion	0.7795	0.7744	Non fickian
F12	0.7348	0.9542	0.9079	Diffusion	0.7795	0.8705	Non fickian

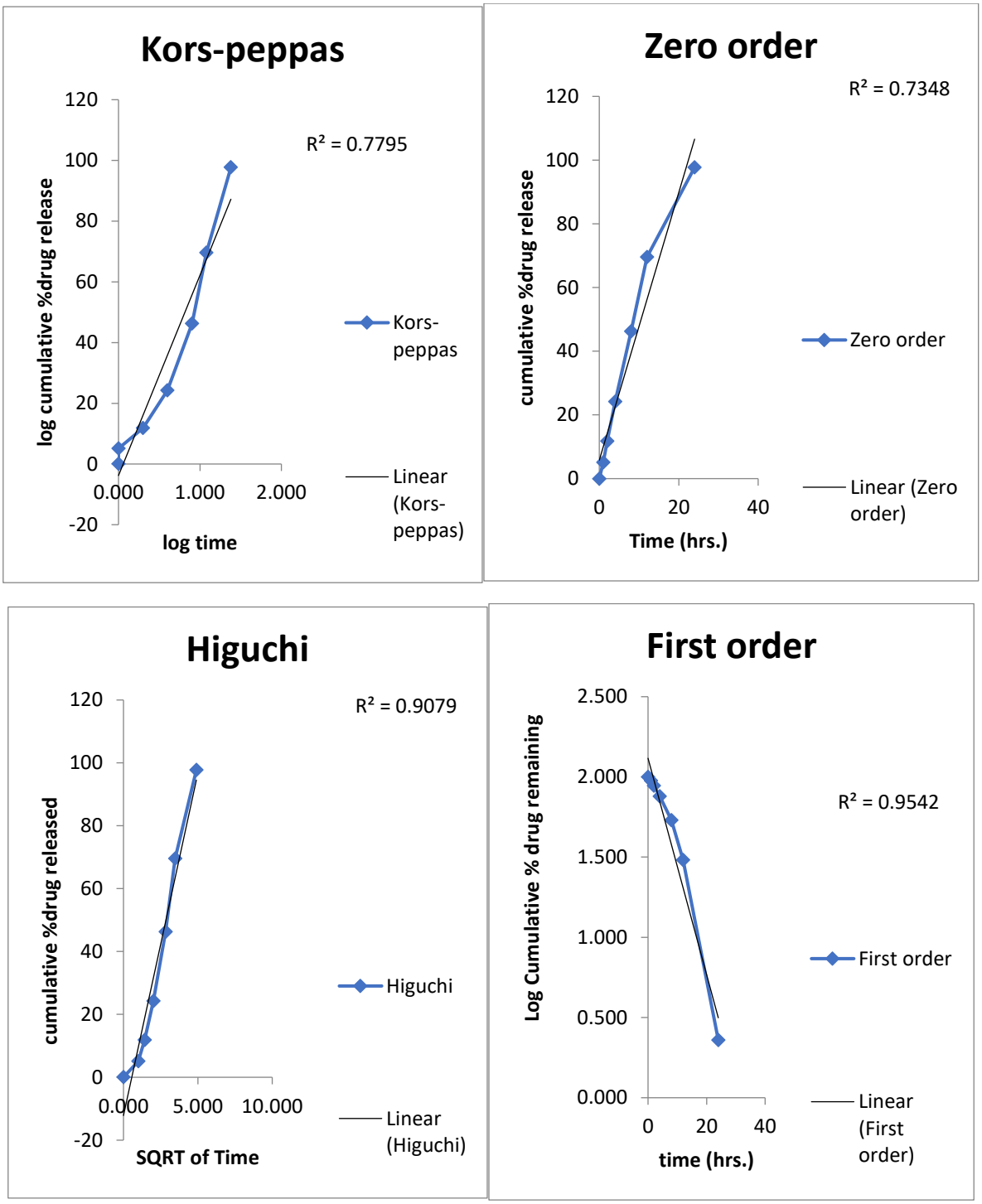

Figure 21: Drug release data of formulation F5 fitting to various kinetic models

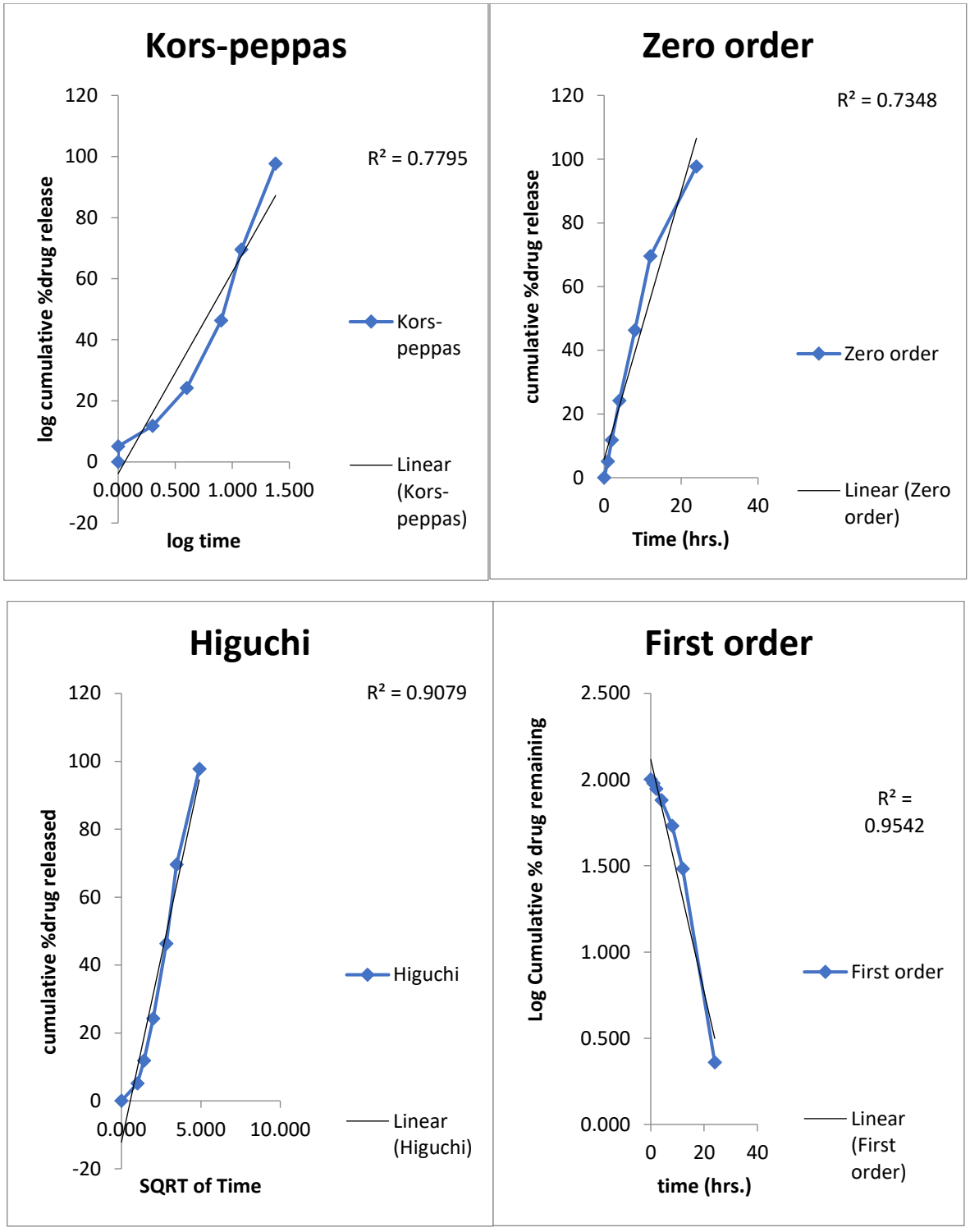

Figure 22: Drug release data of formulation F6 fitting to various kinetic models

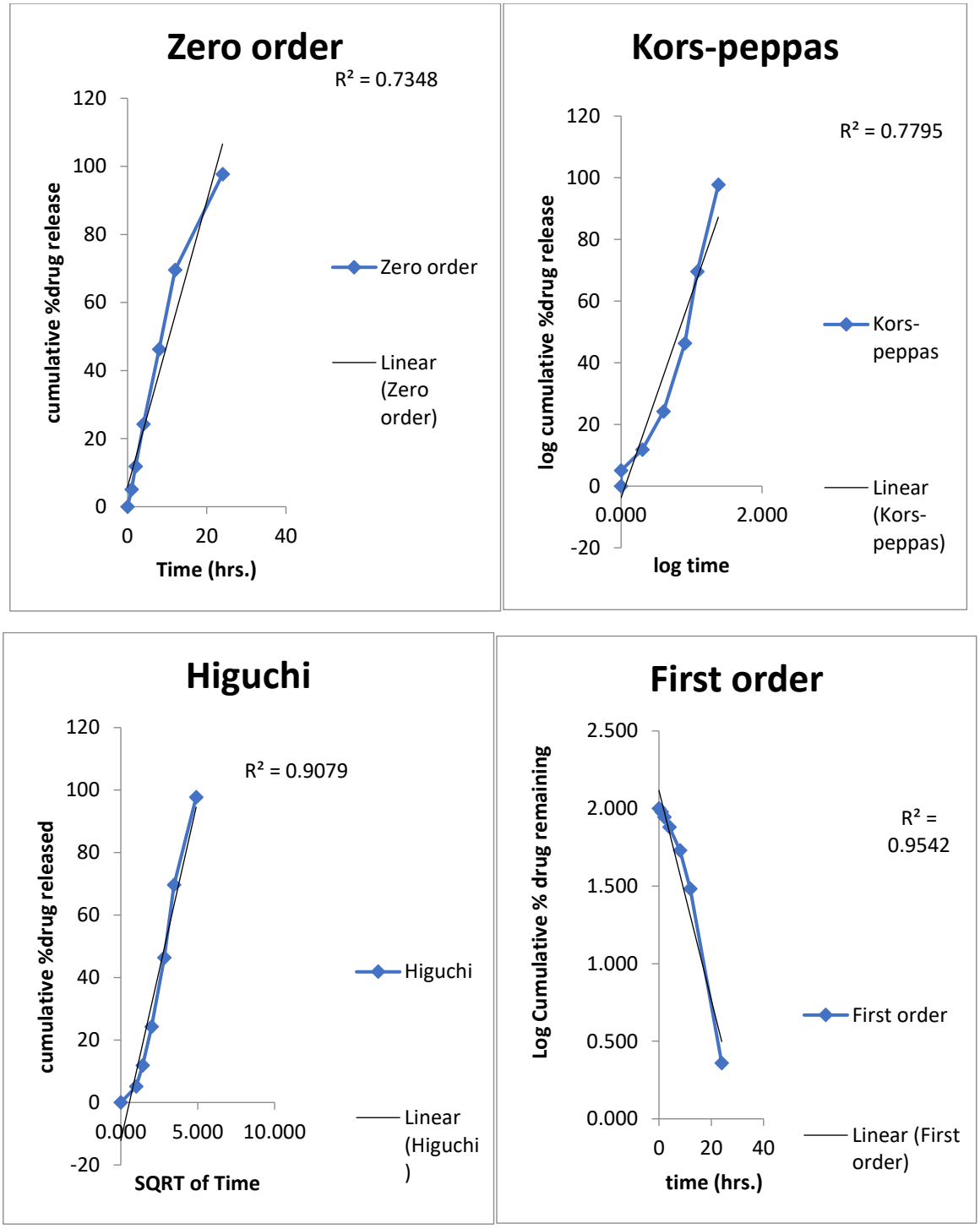

Figure 23: Drug release data of formulation F7 fitting to various kinetic models

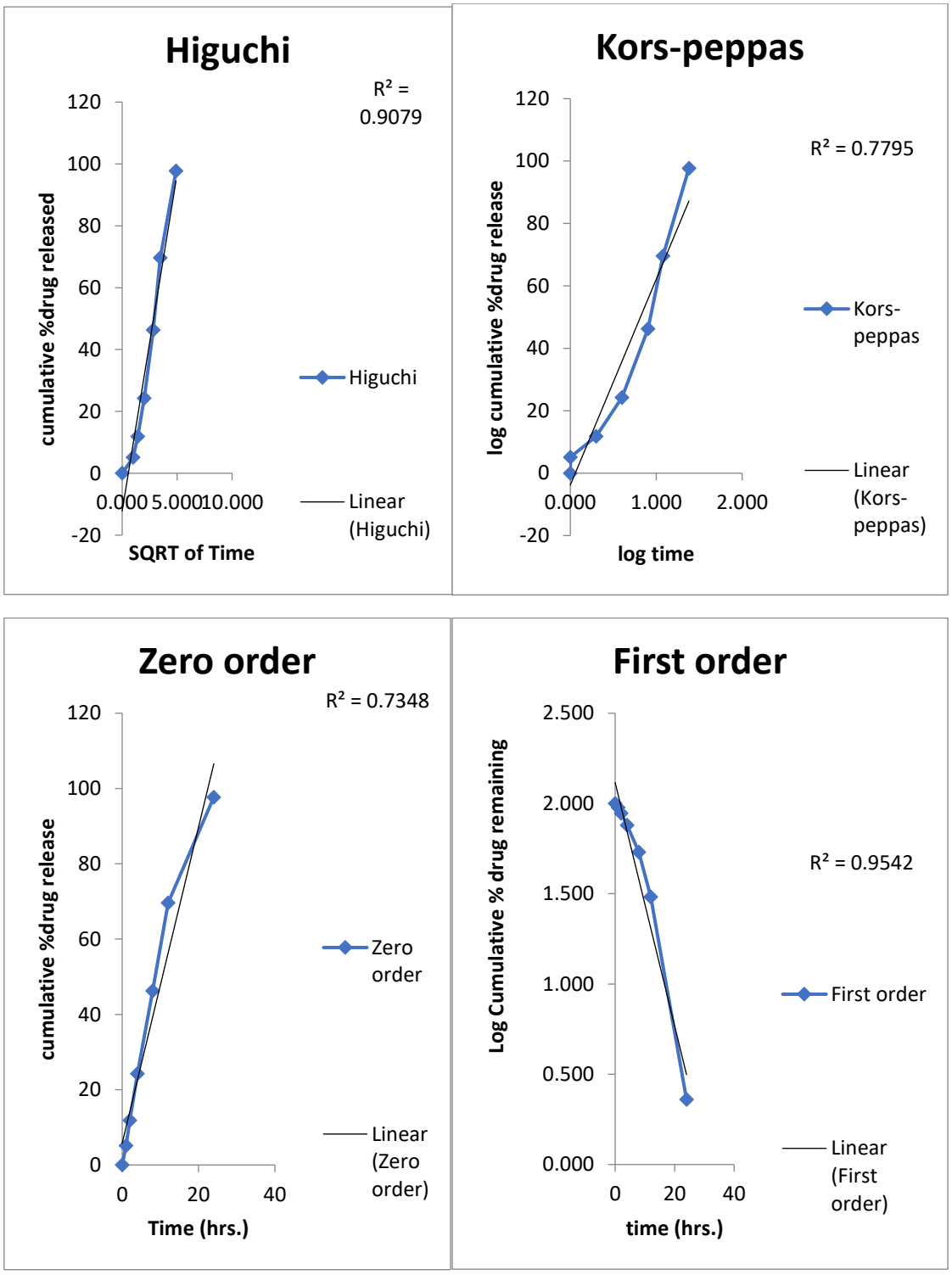

Figure 24: Drug release data of formulation F8 fitting to various kinetic models

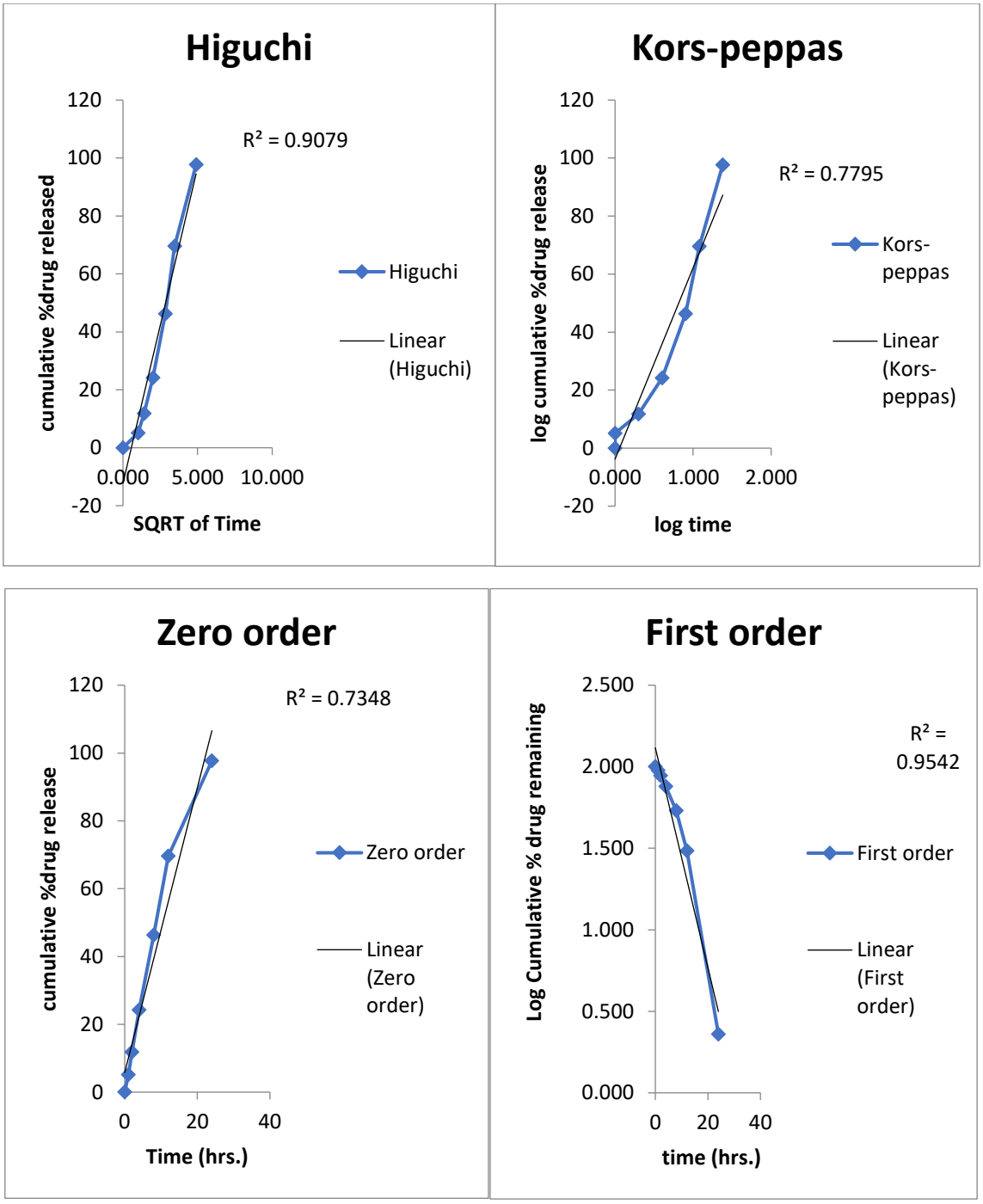

Figure 25: Drug release data of formulation F9 fitting to various kinetic models

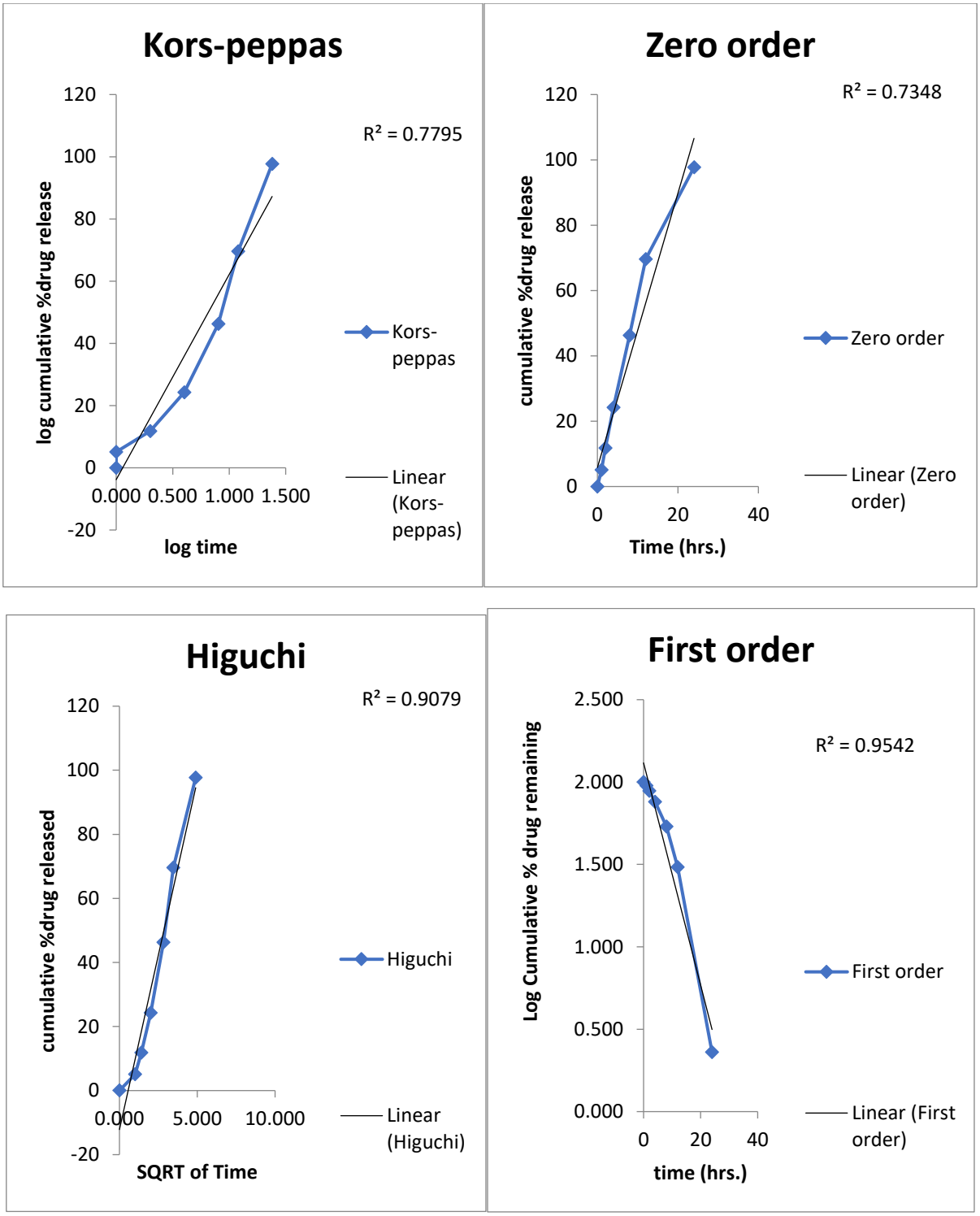

Figure 26: Drug release data of formulation F10 fitting to various kinetic models

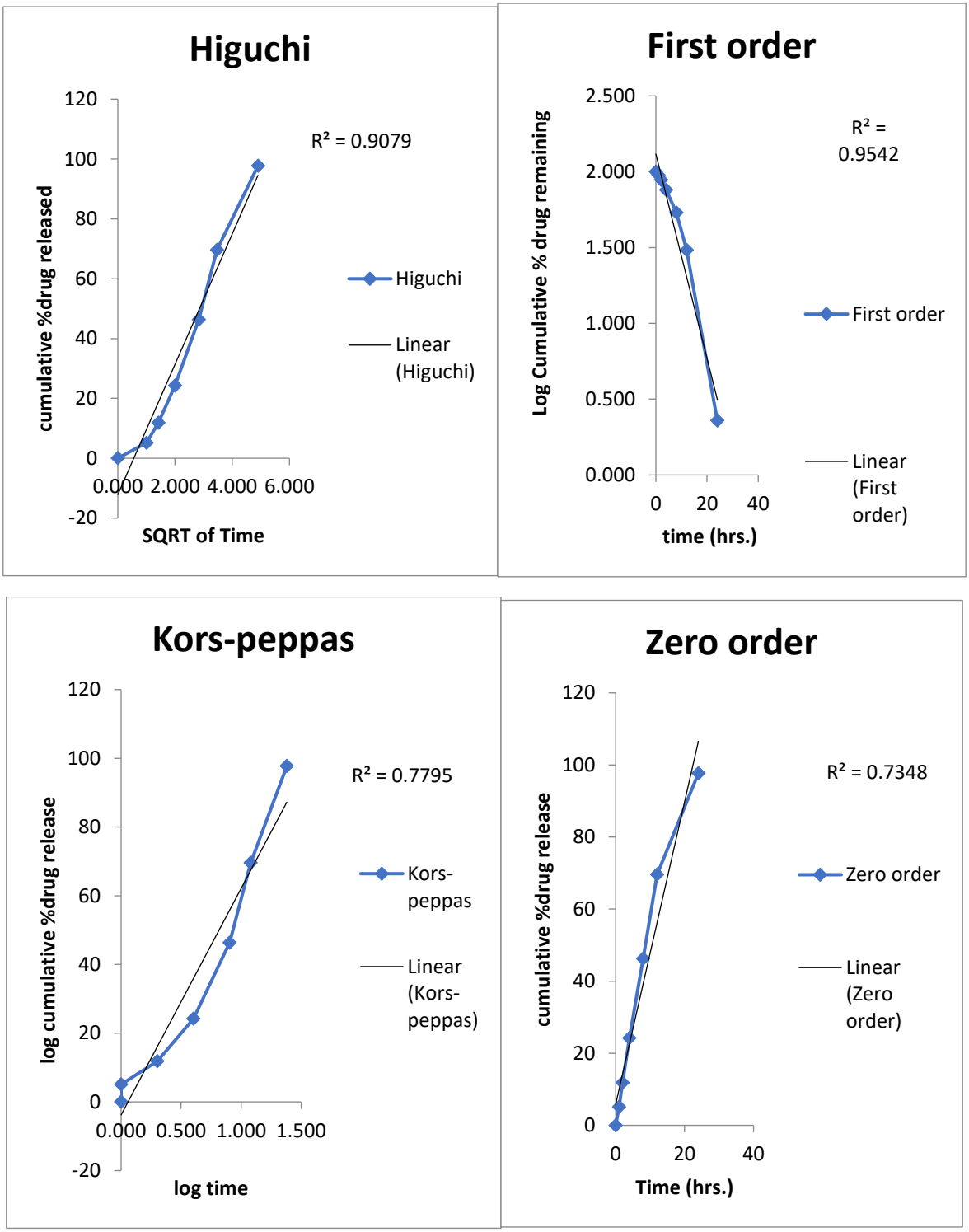

Figure 27: Drug release data of formulation F11 fitting to various kinetic models

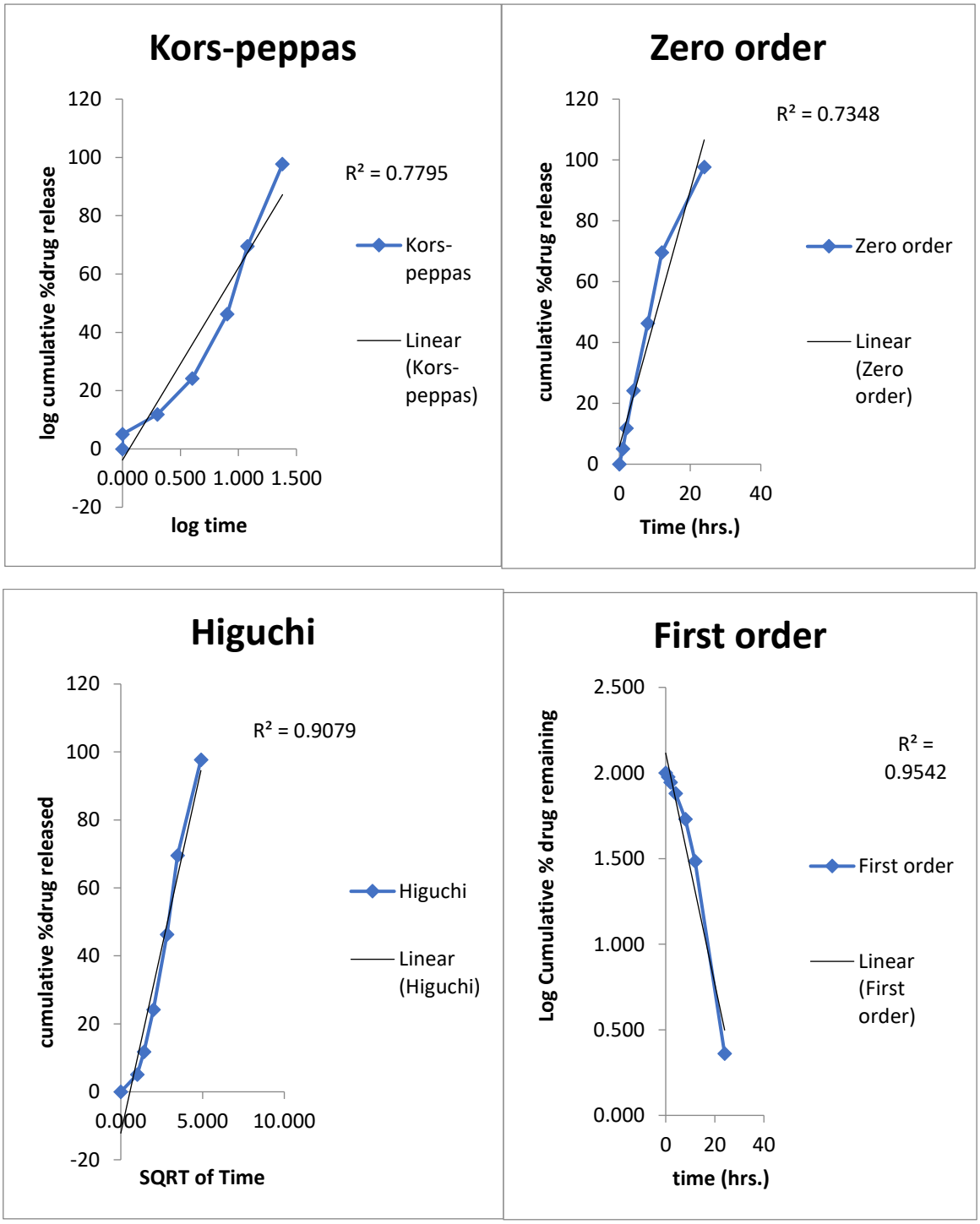

Figure 28: Drug release data of formulation F12 fitting to various kinetic models

Summary & Conclusion

SUMMARY AND CONCLUSION

On March 11, 2020, the WHO declared the COVID-19 outbreak a pandemic. As of May 2020, SARS-CoV-2 has spread across the world in over 185 countries, with millions of infections and hundreds of thousands of deaths. Nanotechnology offers a number of solutions to fight viruses, both outside and inside the host, and several nanotechnology-based platforms have already been successful in preclinical studies to counter several human viral pathogens such as HIV, human papilloma virus, herpes simplex, and respiratory viruses.

Magnetic nanoparticles (MNPs) which exhibit para magnetism in the absence of external magnetic field. However, MNPs display super-para magnetism in the presence of magnetic field which helps to target at particular site by using external magnet as it contain exceptional optical, electrical and chemical properties which permit their applications in virus detection, magnetic cell separation, enzyme catalysis, gene therapy, targeting chemotherapy, radiotherapy, diagnostics, therapeutics, bio-sensing and information storage. Magnetic nanoparticles exhibiting such properties offer vast advantages over traditional macro or microparticles in targeted drug delivery and treatment.

Silymarin, a potential phytochemical compound obtained from the seeds of *Silybum marianum* (milk thistle) plant has been used as a hepatoprotective agent, and shows strong anti-oxidant effect. Now evidence suggests that the extract possesses potent antiviral activities against numerous viruses, particularly hepatitis C virus (HCV). Consequently, silymarin is the most commonly consumed herbal product among HCV-infected patients in western countries. Antiviral efficacy of silymarin has also been reported against human papillomavirus, a highly carcinogenic virus. Various antiviral activities of silymarin and derivatives have been shown against liver and non-liver pathogens, making them potential broad-spectrum antivirals, for some of the enveloped viruses explored to date. The high incidence of administration of silymarin together with its short half-life and poor bioavailability proposed great scope for the proposal of nanoparticulate drug delivery systems.

The aim and objective of this project is to contribute towards covid-19 and also target the affected site of lung for better bioavailability and to reduce the further toxicity. The binding ability of silymarin with the receptor was assessed by comparing to the standard drug Remdesivir by molecular docking. In this present work silymarin magnetic nanoparticle has been formulated with three different types of polymers (Ethyl cellulose, Eudragit, Polyethylene glycol) by co- precipitation method.

Molecular docking study was carried out to evaluate the most preferred geometry of the protein ligand complex. Homosapien covid receptors were used for performing docking study as target proteins. Various Homosapien receptor were selected and docked. The best binding receptors were further compared with the standard ligand. Remdesivir is the selected standard as it is the most potent currently used Anti-viral drug. Among various Covid -19 receptors docked, 5N11, 7JMP,7JMO with -8.09, -7.23, -6.96 has showed more binding ability towards silymarin then that of the standard drug Remdesivir.

Preformulation studies were carried out to find out the solubility of Silymarin. Solubility test gave an idea that silymarin is not water soluble but soluble in solvents like acetone, dichloromethane etc.

FTIR and UV spectral studies authenticate the spectra obtained with the sample drug matched with standard pure drug. UV spectra gave the maximum absorption peak at 288nm.The comparison of FTIR spectra of Silymarin and mixture of Silymarin and polymer confirms that there is no appearance of additional new peaks and disappearance of existing peaks from that of the drug. This indicates that there is no interaction between the drug and polymer used in the study.

Super Paramagnetic Iron Oxide Nanoparticle (SPIONs) was carried out by Co-precipitation method. This method was simple and cost effective. The percentage yield is low in formulation F1,F2,F3 and F4 ie, below 30% and high in formulation F5, F6, F7 and F8 (78.16 %). It can also be noted that the yield obtained while using ethyl cellulose as polymer is much higher when compared with eudragit and polyethylene glycol. Since the yield is less in formulations F1-F5 with Eudragit, they are not considered for further studies.

The entrapment efficiency was found to be highest for F8 formulation (Silymarin: ethyl cellulose, ratio 1:2) which is 96.43% and the lowest entrapment of drug was found for F11 formulation (Silymarin: polyethylene glycol ratio 1:2) which is 80.15%**.** Since the entrapment efficiency is high 96.43% and particle size is less 319 nm for formulation F8 among other formulation, it is considered for Zeta potential measurement and SEM analysis.

Scanning electron micrograph of the prepared magnetic nanoparticle at different magnification showed that the nanoparticle were polydispersed spherical shape. The spherical and polydispersed nature of magnetic nanoparticle was clearly observed in the SEM images.

Particle size and zeta potential was determined by Malvern Zeta sizer. The particle size analysis confirmed that the prepared sample were in the nanometre range. Average particle size

obtained for the formulation ethyl cellulose F8 was found to be 319 nm. Zeta potential values of magnetic nanoparticle indicated that the formulated magnetic nanoparticle is stable.

From the *in-vitro* release data from the dialysis bag diffusion method it was found that formulations F5, F6, F7, F8, F9, F10, F11 and F12 showed the drug release of 111.26, 98.26, 91.12, 94.12,98.78, 99.78, 99.31 and 97.71 respectively at the end of 24 hours. *In-vitro* drug release data indicates that both hydrophobic polymer ethyl cellulose and poly ethylene glycol have sustained the release of drug. There is no significant effect in polymer type. Drug release was observed as a function of drug: polymer ratio type. It was observed that the drug release decreased with the increase in the amount of polymer for each formulation of ethyl cellulose and polyethylene glycol. This is due to the drug release is retarded with the difficulty of the drug to diffuse in the increased swollen matrix of the polymer with the higher concentration.

The data obtained from the *in vitro* release study was fitted to the models which were used to find out the mechanism of drug release from silymarin magnetic nanoparticle. The *in vitro* release model best fitted to Higuchi release order. This was confirmed by plotting percentage cumulative drug release and square root of time and r^2 value ranges between 0.8477 and 0.9888.

CONCLUSION

The Silymarin magnetic nanoparticle can be formulated by cost effective and easy co-precipitation method using polymers such as ethyl cellulose, eudragit and polyethylene glycol. The formulated silymarin magnetic nanoparticle can be used in the treatment of Covid-19 as it has shown higher binding ability compared to Remdesivir. This can be targeted to the particular site of affected area of lung which in turn reduces the dose, frequency of administration and the side effects. This formulation can be better treatment for Covid-19.

References

REFERENCE

1. Valamla Bhavanaa , Pradip Thakora , Shashi Bala Singhb and Neelesh Kumar Mehra. COVID-19: Pathophysiology, treatment options, nanotechnology approaches, and research agenda to combating the SARS-CoV2 pandemic. *Life Sciences*.2020; 18336: 261
2. Eduardo Ruiz-Hitzky, Margarita Darder, Bernd Wicklein, Cristina Ruiz-Garcia, Raquel Martín-Sampedro, Gustavo del Real *et.al*. Nanotechnology Responses to COVID-19. *Advance Healthcare Material*.2020; 2000979: 1-26
3. Estefânia V. R. Campos, Anderson E. S. Pereira, Jhones Luiz de Oliveira, Lucas Bragança Carvalho, Mariana Guilger-Casagrande, Renata de Lima and Leonardo Fernandes Fraceto. How can nanotechnology help to combat COVID-19? Opportunities and urgent need. *Journal of Nanobiotechnology*.2020; 18:125
4. Carsten Weiss, Marie Carriere, Laura Fusco, Ilaria Capua, Jose Angel Regla-Nava, Matteo Pasquali, James A. Scott *et.al.* Toward Nanotechnology-Enabled Approaches against the COVID-19 Pandemic. *ACS Nano*.2020; https://dx.doi.org/10.1021/acsnano.0c03697
5. Jose prados, Consolación Melguizo, Raul Ortiz , Celia Vélez, Pablo J. Alvarez, Jose L. Arias. et.al. Doxorubicin-Loaded Nanoparticles: New Advances in Breast Cancer Therapy. *Anti-Cancer Agents in Medicinal Chemistry*. 2012; 12:1058-1070.
6. Salman Khan, Syed Mohd. Danish Rizvi , Varish Ahmad , Mohd Hassan Baig , Mohammad Amjad Kamal, Saheem Ahmad *et.al.* Magnetic Nanoparticles: Properties, Synthesis and Biomedical Applications. *Current Drug Metabolism*. 2015; 16: 685-704.
7. Nima Hamziana, Maryam Hashemib, Mahdi Ghorbanic, Mohammad Hossein Bahreyni Toosid and Mohammad Ramezani. Preparation, Optimization and Toxicity Evaluation of (SPION-PLGA) PEG Nanoparticles Loaded with Gemcitabine as a Multifunctional Nanoparticle for Therapeutic and Diagnostic Applications. *Iranian Journal of Pharmaceutical Research*. 2017; 16 (1): 8-21
8. Ganeshlenin Kandasamy and Dipak Maity. Review Recent advances in superparamagnetic iron oxide nanoparticles (SPIONs) for in-vitro and in-vivo cancer nanotheranostics. *International Journal of Pharmaceutics.* 2015; 496: 191–218. https://doi.org/10.1016/j.ijpharm.2015.10.058.

9. Giovanni Sechi , Davide Bedognetti, Francesco Sgarrella, Laura Van Eperen, Francesco M Marincola, Alberto Bianco and Lucia Gemma Delogu. The perception of nanotechnology and nanomedicine: a worldwide social media study. *Nanomedicine*. 2014; 9: 1475–1486.

10. Nguyen T K Thanh , N Maclean and S Mahiddine. Mechanisms of nucleation and growth of nanoparticles in solution. *Chemical Reviews*. 2014; 114: 7610–7630. http://dx.doi.org/10.1021/cr400544s.

11. S. Vikram, M. Dhakshnamoorthy, R. Vasanthakumari, A. R. Rajamani, Murali Rangarajan and Takuya Tsuzuki. Tuning the magnetic properties of iron oxide nanoparticles by a room-temperature. *Journal of Nanoscience and Nanotechnology*. 2014; 14: 1–9. http://dx.doi.org/10. 1166/jnn.2014.9544.

12. Fong-Yu Cheng , Chia-Hao Su, Yu-Sheng Yang, Chen-Sheng Yeh, Chiau Yuang Tsai, Chao-Liang Wu. et.al. Characterization of aqueous dispersions of Fe3O4 nanoparticles and their biomedical applications. *Biomaterials.* 2005; 26: 729–738, http://dx.doi.org/10.1016/j. biomaterials.2004.03.016.

13. Dipak Maity, Shi-Guang Choo, Jiabao Yi, Jun Ding and Jun Min Xue. Synthesis of magnetite nanoparticles via a solvent-free thermal decomposition route. *Journal of Magnetism and Magnetic Materials.* 2009; 321:1256–1259. http://dx.doi.org/10.1016/j.jmmm.2008.11.013.

14. Xu C, Xie J, Kohler N, Walsh EG, Chin YE and Sun S. Monodisperse magnetite nanoparticles coupled with nuclear localization signal peptide for cell-nucleus targeting. *Chemistry, An Asian Journal*. 2008; 3: 548–552. http://dx.doi.org/10.1002/ asia.200700301.

15. Arjun Prakash , Huiguang Zhu, Christopher J Jones, Denise N Benoit, Adam Z Ellsworth, Erika L Bryant and Vicki L Colvin. Bilayers as phase transfer agents for nanocrystals prepared in nonpolar solvents. *ACS Nano*. 2009; 3: 2139–2146. http://dx.doi.org/10.1021/nn900373b.

16. Yuan Liu ,Tao Chen , Cuichen Wu , Liping Qiu, Rong Hu and Juan Li . Facile surface functionalization of hydrophobic magnetic nanoparticles. *Journal of American Chemical Society*. 2014; 136:12552–12555. http://dx.doi.org/ 10.1021/ja5060324.

17. R.Ramesh, M.Rajalakshmi, C.Muthamizhchelvan and S.Ponnusamy. Synthesis of Fe3O4 nanoflowers by one pot surfactant assisted hydrothermal method and its

properties. Materials Letter. 2012; 70: 73–75. http://dx.doi.org/10.1016/j.matlet.2011.11.085.

18. Yi-Xiang J Wang, Shouhu Xuan, Marc Port and Jean-Marc Idee. Recent advances in superparamagnetic iron oxide nanoparticles for cellular imaging and targeted therapy research. Current Pharmaceutical Design. 2013; 19: 6575–6593.
19. Chuka Okoli, Magali Boutonnet, Laurence Mariey, Sven Järås and Gunaratna Rajarao. Application of magnetic iron oxide nanoparticles prepared from microemulsions for protein purification. Journal of Chemical Technology and Biotechnology. 2011; 86: 1386–1393. http://dx.doi.org/10.1002/ jctb.2704.
20. Chuka Okoli , Margarita Sanchez-Dominguez, Magali Boutonnet, Sven Järås, Concepción Civera, Conxita Solans and Gunaratna Rajarao Kuttuva. Comparison and functionalization study of microemulsion prepared magnetic iron oxide nanoparticles. *Langmuir*. 2012; 28: 8479–8485.
21. Chin A.B and Yaacob.Synthesis and characterization of magnetic iron oxide nanoparticles via w/o microemulsion and Massart's procedure. *Journal of Materials Processing Technology*. 2007; 191: 235–237.
22. ReymanDolores, SerranoRaquel and Garcia-LeisAdianez.Sonochemical synthesis of iron oxide nanoparticles loaded with folate and cisplatin: effect of ultrasonic frequency, Ultrasonic Sonochemistry. 2015; 23: 391–398. http://dx.doi.org/10.1016/j.ultsonch.
23. Oana pascu, elisa carenza, martí gich, sonia estradé, f. Peiró, gervasi herranz and anna roig. Surface reactivity of iron oxide nanoparticles by microwave-assisted synthesis; comparison with the thermal decomposition route. *The Journal of Physical Chemistry*. 2012; 116: 15108–15116.
24. ElisaCarenza, VerónicaBarceló, AnnaMorancho, JoanMontaner, AnnaRosell and AnnaRoig. Rapid synthesis of water-dispersible superparamagnetic iron oxide nanoparticles by a microwave-assisted route for safe labeling of endothelial progenitor cells. *Acta Biomaterialia*. 2014; 10: 3775–3785. http://dx.doi.org/10.1016/j.actbio.
25. Hyejung Mok and Miqin Zhang, Superparamagnetic Iron Oxide Nanoparticle-Based Delivery Systems for Biotherapeutics. *Expert Opinion Drug Delivery*. 2013;10(1): 73–87. doi:10.1517/17425247.2013.747507.
26. Iqra Qaddir, Nouman Rasool, Waqar Hussain and Sajid Mahmood. Computer-aided analysis of phytochemicals as potential dengue virus inhibitors based on molecular docking, ADMET and DFT studies. *Journal of Vector Borne Diseases*.2017; 255–262

27. Ching-Hsuan Liu, Alagie Jassey, Hsin-Ya Hsu and Liang-Tzung Lin. Antiviral Activities of Silymarin and Derivatives. *Molecules*. 2019;1552:1-15.
28. Katharina Esser-Nobis, Ines Romero-Brey,Tom M. Ganten, Jerome Gouttenoire, Christian Harak and Rahel Klein.et. al. Analysis of Hepatitis C Virus Resistance to Silibinin InVitro and InVivo Points to a Novel Mechanism Involving Nonstructural Protein 4B. *Hepatology*. 2013; 953-963.
29. Jianjun Zheng , Wenzhi Ren, Tianxiang Chen, Yinhua Jin1, Aijing Li1 , Kun Yan *et.al.* Recent Advances in Superparamagnetic Iron Oxide Based Nanoprobes as Multifunctional Theranostic Agents for Breast Cancer Imaging and Therapy. *Current Medicinal Chemistry*. 2018; 25: 3001-3016.
30. M. Khalkhali, S. Sadighian, K. Rostamizadeh, F. Khoeini, M. Naghibi, 2N. Bayat and M. Hamidiet. Simultaneous diagnosis and drug delivery by silymarin-loaded magnetic nanoparticles. *Nanomedicine*. 2015; 2(3):223-230.
31. Irfan M. Saiyyad, D.S. Bhambere and Dr. Sanjay Kshirsagar.Formulation and Optimization of Silymarin Loaded PLGA Nanoparticle for liver targeting. *Asian Journal of Pharmacy and Technology*. 2017; Vol. 7: Issue 4 ,209-220.
32. Prashanth K.B. Nagesh, Nia R. Johnsona, Vijaya K.N. Boyaa, Pallabita Chowdhurya, Shadi F. Othmanb, Vahid Khalilzad-Sharghi.et.al. PSMA targeted docetaxel-loaded superparamagnetic iron oxide nanoparticles for prostate cancer. *Colloids Surfaces B: Biointerfaces*. 2016; 144: 8–20. doi:10.1016/j.colsurfb.2016.03.071.
33. H. Kouchakzadeh, Hoseini Makarem, S.A. Shojaosadati. Simultaneous loading of 5-florouracil and SPIONs in HSA nanoparticles: Optimization of preparation, characterization and in vitro drug release study. *Nanomedicine*.2015; 3(1): 35-42.
34. Frederic Tewes, Carsten Ehrhardt and Anne Marie Healy. Superparamagnetic iron oxide nanoparticles (SPIONs)-loaded Trojan microparticles for targeted aerosol delivery to the lung. *European Journal of Pharmaceutics and Biopharmaceutics*.2015; 86:98-104.
35. Meijia wu and shengwu huang. Magnetic nanoparticles in cancer diagnosis, drug delivery and treatment (Review). *Molecular and Clinical Oncology*.2017; 7: 738-746.
36. Soumaye Amirsaadat, Younes Pilehvar-Soltanahmadi, Faraz Zarghami, Shahriar Alipour, Zohreh Ebrahimnezhad and Nosratollah Zarghami. Silibinin-loaded magnetic nanoparticles inhibit hTERT gene expression and proliferation of lung cancer cells.

Artificial Cells, Nanomedicine, and Biotechnology. 2017; 1-8. http://dx.doi.org/10.1080/21691401.2016.1276922.

37. Arun R. Raj. Formulation and evaluation of prednisolone tablets using biodegradable natural polysaccharides as a carrier in colon targeted drug delivery. *International Journal of Pharmaceutical Sciences and Research*. 2013; Vol. 4(6): 2274-2279.
38. Nidhi Mishra, Prerna Pant, Ankit Porwal, Juhi Jaiswal, Mohd. Aquib Samad and Suraj Tiwari. Targeted Drug Delivery: A Review. *American Journal of PharmTech Research*. 2016; 6(1) ISSN: 2249-3387.
39. Hung-Wei Yang, Mu-Yi Hua, Hao-Li Liu, Chiung-Yin Huang and Kuo-Chen Wei. Potential of magnetic nanoparticles for targeted drug delivery. *Nanotechnology, Science and Applications.* 2012; 5: 73–86.
40. Mansour Binandeh. Coronavirus Destruction (Covid-19), with High Efficacy of Magnetic Nanoparticles Containing Antiviral Drug Favipiravir/Remdesivir. *Journal of Bioanalysis & Biomedicine*. 2021; Special Issue S6: 249
41. Subashini Rajaram, Anjuna Prakashan, B. Pragathi, K. Saieswari, A. R. V. Sree and Yashoda Mariappa Hedge. The potential role of nanotechnology to combat SARS-COV2 -2019: diagnosis, treatment options, approaches – a scopious review. *International Journal of Pharmaceutical Sciences and Research*. 2021; Vol. 12(6): 2966-2981.
42. Gabriela Palestino, Ileana García-Silva, Omar González-Ortega and Sergio Rosales-Mendoza. Can nanotechnology help in the fight against COVID-19?. *Expert review of anti-infective therapy.* 2020; vol.18 (9): 849–864.
43. Malobika Chakravarty and Amisha Vora. Nanotechnology-based antiviral therapeutics. *Drug Delivery and Translational Research*.2020; https://doi.org/10.1007/s13346-020-00818-0
44. Swati Gupta, Shailendra Kumar Singh and Priti Girotra. Targeting silymarin for improved hepatoprotective activity through chitosan nanoparticles. *International Journal of Pharmaceutical Investigation*. 2014; Vol 4: 156-163.
45. Asif Mir, Syeda Naqsh e Zahra and Sobiah Rauf. Comparative Modeling and Molecular Docking Study of P53 and AKT1, Genes of Lung Cancer Pathways. *International Journal of Clinical Oncology and Cancer Research*.2016;1(1): 6-14.

46. Syed Aun Muhammad and Nighat Fatima. In silico analysis and molecular docking studies of potential angiotensin-converting enzyme inhibitor using quercetin glycosides. *Pharmacognosy Magazine*. 2015; Vol 11, Issue 42 :123-126.
47. Wen-Chan Hsu, Lean-Teik, Tzu-Hui Wu, Liang-Tzung Lin, Feng-Lin Yen, and Chun-Ching Lin. Characteristics and Antioxidant Activities of Silymarin Nanoparticles. Journal of Nanoscience and Nanotechnology. 2012; Vol. 12: 2022–2027.
48. Nemany A.N.Hanafy and Maged A. El-Kemary. Silymarin/curcumin loaded albumin nanoparticles coated by chitosan as muco-inhalable delivery system observing anti-inflammatory and anti-COVID-19 characterizations in oleic acid triggered lung injury and in vitro COVID-19 experiment. *International Journal of Biological Macromolecules*. 2022; 198:101–110
49. Suvadra Das, Partha Roy, Runa Ghosh Auddy and Arup Mukherjee. Silymarin nanoparticle prevents paracetamol-induced hepatotoxicity. *International Journal of Nanomedicine.*2011;6 :1291–1301.
50. Hyejung Mok and Miqin Zhang. Superparamagnetic Iron Oxide Nanoparticle-Based Delivery Systems for Biotherapeutics. *Expert Opinion on Drug Delivery*. 2013; 0(1): 73–87. doi:10.1517/17425247.2013.747507.
51. Farshad Yazdani and Mahdieh Seddigh. Magnetite nanoparticles synthesized by co-precipitation method: The effects of various iron anions on specifications. *Materials Chemistry and Physics*. 2016;184:318-323
52. Sarasambi SP, Anupama K, Kalyan K and Malipatil S.M. Study of Spectrophotometric Estimation of Silibilin in Bulk Drugs and its Pharmaceutical Formulation. Asian Journal of Biochemical and Pharmaceutical Research.2011; 2(1): 213-219.
53. Indian pharmacopeia 2014
54. Thamaraiselvi, t. Selvankumar, G. Wesely and v. K. Nathan. In Silico Molecular Docking on Bioactive Compounds from Indian Medicinal Plants against Type 2 Diabetic Target Proteins: A Computational Approach. *Indian Journal of Pharmaceutical Sciences.*2021;1273-1279.
55. Syed Aun Muhammad and Nighat Fatima. In silico analysis and molecular docking studies of potential angiotensin-converting enzyme inhibitor using quercetin glycosides. *Pharmacognosy Magazine*.2015; Vol 11.

56. Priyanka D, Sindhu S, Maanvizhi S. Design Development and Evaluation of Ibuprofen Loaded Nanosponges for Topical Application. *International Journal of Chemtech Research*. 2018; 11(02): 218-227.
57. Iida, H, Takayanagi, K, Nakanishi T, Osaka T. Synthesis of Fe3O4 nanoparticles with various sizes and magnetic properties by controlled hydrolysis. *Journal of Colloid and Interface Science.* 2007; 314:274-280.